STUDY OF SWITCHING OVERVOLTAGES ON TRANSMISSION LINES

A Thesis Submitted
In Partial Fulfilment of the Requirements
for the Degree of

MASTER OF TECHNOLOGY

by

PRODIP KUMAR CHOWDHURY

to the

DEPARTMENT OF ELECTRICAL ENGINEERING
INDIAN INSTITUTE OF TECHNOLOGY, KANPUR
SEPTEMBER, 1984

Dedicated to

my

Parents

CERTIFICATE

This work entitled 'STUDY OF SWITCHING OVERVOLTAGES ON TRANSMISSION LINES" by Prodip Kumar Chowdhury has been carried out under our supervision and this has not been submitted elsewhere for a degree.

Dr. Ravindra Arora
Assistant Professor

Dr. Rakosh Das Begamudre
Visiting Professor

Department of Electrical Engineering
Indian Institute of Technology
Kanpur 208016.

ACKNOWLEDGEMENTS

I wish to express my deepest sense of gratitude to Dr. Rakosh Das Begamudre and Dr. Ravindra Arora who initiate the problem and provided valuable guidance without which thi thesis would not have been completed.

I am highly obliged to Dr. L.P. Singh for his consta encouragements throughout the course of this work.

I am thankful to the authorities of Central Power Research Institute (CPRI), Bangalore for having granted me t permission to carry out some experiments in their High Voltag Research and Development Division. I am extremely grateful t Mrs. Sujatha Subhash and Mrs. K.S. Meera of the CPRI Bangalo for their help and suggestions in performing the experiments.

I am greatly indebted to Sivakumar and Islam for thei help during the final stages of this work. I thank my friend Ashish, Srikanth, Reddy, Swarup, Chakravorty, Deshpande, Muku and Kailash Nath who made my stay in this Institute a pleasan and a memorable one.

Finally, a special word of thanks to my friend Senthi for his help to bring this thesis to its final shape and for his constant encouragement during my stay at I.I.T. Kanpur. Thanks are due to Mr. R.N. Srivastava for his fast and efficient typing.

- PRODIP KUMAR CHOWDHURY

CONTENTS

LIST OF PRINCIPAL SYMBOLS

R_o : Zero sequence resistance of the line per km

R_1 : Positive sequence resistance of the line per km

L_o : Zero sequence inductance of the line per km

L_1 : Positive sequence inductance of the line per km

C_o : Zero sequence capacitance of the line per km

C_1 : Positive sequence capacitance of the line per km

w : System frequency

E_g : Source voltage

E_o : Sending end bus voltage

V : Receiving end bus voltage

Z_g : Source impedance

L_g : Source inductance

R_g : Source resistance.

ABSTRACT

In this thesis, switching transient overvoltages occurring on 3-phase 220 kV and 400 kV transmission lines have been calculated using a generalised computer program developed. For the 220 kV line, the theoretical results obtained from the digital calculations have also been compared with model studies, using Transient Network Analyser (TNA). Studies of switching overvoltages have been carried out for unloaded lines, for simple line terminations and for transformer terminated lines. The effect of source impedance, line length and the simultaneous and non-simultaneous closure of circuit breakers have been studied. Switching surge control by using pre-insertion resistors and shunt reactor compensation have also been investigated.

CHAPTER 1

INTRODUCTION

With the increase in power demand and the economic necessities to locate generating stations in remote areas, the present trend is to transmit the bulk power over long distance extra high voltage (EHV) lines. In an EHV system, the insulation level is mainly determined by overvoltages caused due to switching [3, 13, 15]. A poor choice of insulation level will either increase the cost of the system or will increase risk of failures due to faults initiated by flashovers. Therefore a proper insulation level should be chosen which requires the knowledge of the nature and magnitudes of switching overvoltages produced due to different system conditions. Also, an understanding of switching overvoltage is of importance for the design of lightning arresters, circuit breakers, and for the operation of protective relays. Since the magnitude and time duration of various switching overvoltages is different, therefore, they stress the insulation in different manner.

It is technically and economically desirable to control the switching overvoltages appearing on transmission lines. This can be achieved by using lightning arresters, shunt reactor compensation and preinsertion resistors or by synchronous closure of circuit breakers. The most effective means for achieving a substantial reduction in

switching overvoltage is by using pre-insertion resistors across the main circuit breaker contacts.

The following methods are available to study the switching-surge overvoltage problem in power-system

(i) Digital computer calculation

(ii) Model studies on a transient network analysis (TNA)

(iii) Field testing and

(iv) Insulation testing in the laboratory.

In this work an attempt has been made to study the phase to neutral and phase to phase switching overvoltages under different system conditions for the 220 kV and 400 kV lines using the digital computer program developed. Switching surge control by using pre-insertion resistors and shunt reactor compensation and their effects on the switching surge magnitude have also been investigated. Experiments have also been performed on the Transient Network Analyser on three phase basis for the simulated 220 kV lines available at CPRI, Bangalore.

Chapter 2 deals with the design of coils for transmission line model for different system voltage levels. The phase to neutral switching overvoltage for unloaded lines, for resistive and inductive load terminated lines, transformer terminated lines and for lines terminated in R-L-C combinations have been observed on the TNA. The effect of source impedance, line length, shunt reactor compensation and transformer winding connections have also been studied.

In Chapter 3, the phase to neutral switching overvoltages for 220 kV and 400 kV line have been calculated for different system conditions by using the digital computer program developed. The different system conditions that were considered are unloaded lines, lines with resistive- and inductive-load and transformer terminated lines. Switching surge control by using pre-insertion resistors and shunt reactor compensation have also been investigated. The results of digital computer calculations for the 220 kV line have been compared with the results obtained from the Transient Network Analyser.

In Chapter 4, the phase to phase switching overvoltage of the 400 kV lines have been calculated for different system conditions. For the 220 kV lines, the phase to phase overvoltages were observed on the TNA.

Chapter 5 gives the conclusions drawn from the work done in this thesis.

CHAPTER 2

TNA STUDY ON PHASE TO NEUTRAL SWITCHING OVERVOLTAGE

2.1 Introduction:

For the design, planning, control and analysis of power systems, it is necessary to know the conditions which give rise to different transient behaviour due either to normal and abnormal operations and to have means for calculating the effect of these behaviours on the system. In conducting such studies, the Transient Network Analyser (TNA) has been recognised as a useful tool. This gives a preliminary idea in designing and selecting suitable range of instruments for conducting field tests. The digital computer calculations can also be checked with the results obtained from the TNA.

In this chapter, coils for representing the U.P. 400 kV line and the 735 kV lines have been designed. By connecting a number of Pi-sections, a transmission line model was built and the step response of this model has been compared with the step response calculated for distributed-parameter lines by using the Travelling wave method. The step response for different system conditions have also been observed.

TNA experiments by using three phase sinusoidal excitatin whose point of switching can be varied were performed on the available 220 kV three-phase transmission line models at CPRI Bangalore, representing lines of 100 km and 250 km lengths. The phase to neutral switching

overvoltages of unloaded, resistive-loaded, inductive-loaded, transformer terminated and R-L-C terminated lines have been investigated. The effect of short-circuit power, line length, shunt reactor compensation as well as the transformer winding connections on the switching overvoltage has also been studied.

2.2 Design of Coil for Transmission Line Model:

The parameters of transmission lines although of distributed nature, are represented approximately by the use of models comprised of resistors, inductors and capacitors. In order to accurately represent a long transmission line for studying transient disturbances on TNA, a sufficient number of Pi-sections are provided so that the results are acceptable. The most expensive portion of a transmission line model is the large number of coils required for representing the inductance and resistance of the line. These coils, when connected in a series of Pi-sections will simulate almost the same transient performance of a long line having distributed parameters. An air core coil has been found most suitable for representing the inductance and resistance for transient study [1]. The series elements of line resistance and inductance that have been used for the line model are the positive sequence parameters.

Calculation of inductance and capacitance for line representation is based on equations (B.1) to (B.6) given in Appendix-B. The design of coil for representing the resistance and inductance is based on Brook's coil representation [1].

Calculation of the dimensions of the coil have been carried out according to the details given in Appendix-C.

The results of calculation of line parameter and the dimensions of the coil, for different line configurations, as given in Appendix-A, are given in Tables 1 and 2 respectively.

Table 1

Line parameter for the U.P. 400 kV line and the 735 kV lines

Transmission voltage, kV	:	400	735
Self inductance, mH/km	:	1.14	0.973
Mutual inductance, mH/km	:	0.148	0.117
Positive sequence inductance, mH/km	:	0.992	0.856
Self capacitance, nF/km	:	10.087	11.76
Mutual capacitance, nF/km	:	-1.168	-1.27
Positive sequence capacitance, nF/km	:	12.255	13.03
DC resistance, ohm/km	:	0.028	0.0165

2.3 Step Response of Ladder Network

A lumped parameter equivalent circuit is generally used to represent the actually distributed parameters of the transmission line for transient studies.

A three-phase transmission line model formed by connecting 12 Pi-sections in each phase was built in the laboratory for system studies by using air core coils. The

Table 2

Details of coils for representing U.P. 400 kV and the 735 kV lines

(a) 400 kV line

Length of line per coil, km	10	15	20	25	30
DC resistance, ohm	0.284	0.426	0.568	0.71	0.85
Positive sequence inductance, mH	9.92	14.88	19.84	24.81	29.77
Major dimension, cm	5.29	5.29	5.29	5.29	5.29
Diameter of wire, cm	0.321	0.291	0.269	0.255	0.244
Number of turns	271	330	386	430	470
Length of wire, m	135.11	164.93	192.44	214.38	234.32

(b) 735 kV line

Length of line per coil, km	20	30	40	50
DC resistance, ohm	0.331	0.496	0.662	0.827
Positive sequence inductance, mH	17.31	25.69	34.25	42.82
Major dimension, cm	6.43	6.43	6.43	6.43
Diameter of wire, cm	0.358	0.323	0.301	0.284
Number of turns	322	396	456	512
Length of wire, m	195	240	276	310

line resistance and inductance that have been used for the line model are the positive sequence parameters. The results of step response obtained using this model were compared with the analytical results obtained using the Travelling-wave method.

The voltage waveforms at the receiving end of an open ended line, when a step input is applied at the sending end for different numbers of Pi-sections being 1, 2, 3, 4, 6 and 12 are shown in Figures 2.1(a) to 2.1(f) respectively.

The derivation and calculation of step response for distributed parameter line using the Travelling-wave method is done in Appendix-D. The step response obtained by this method is shown in Figure 2.1(f). From Figures 2.1(a) to 2.1(f) it can be seen that as the number of Pi-sections in the ladder network is increased, its response approaches nearly the response of the distributed parameter line.

The overvoltage in the case of step response of an open-ended line is found to be 1.70 p.u. The step responses of open-ended line, line with surge impedance loading and transformer terminated line have also been compared. The transient overvoltage measured on an open-ended line is found to be higher than the other two configurations. In this study the transformer is represented by an equivalent magnetizing inductance and a resistance to account for core losses.

2.4 Overvoltages on Unloaded Line:

It is general practice on power systems to energise a transmission line by closing a circuit breaker at one end

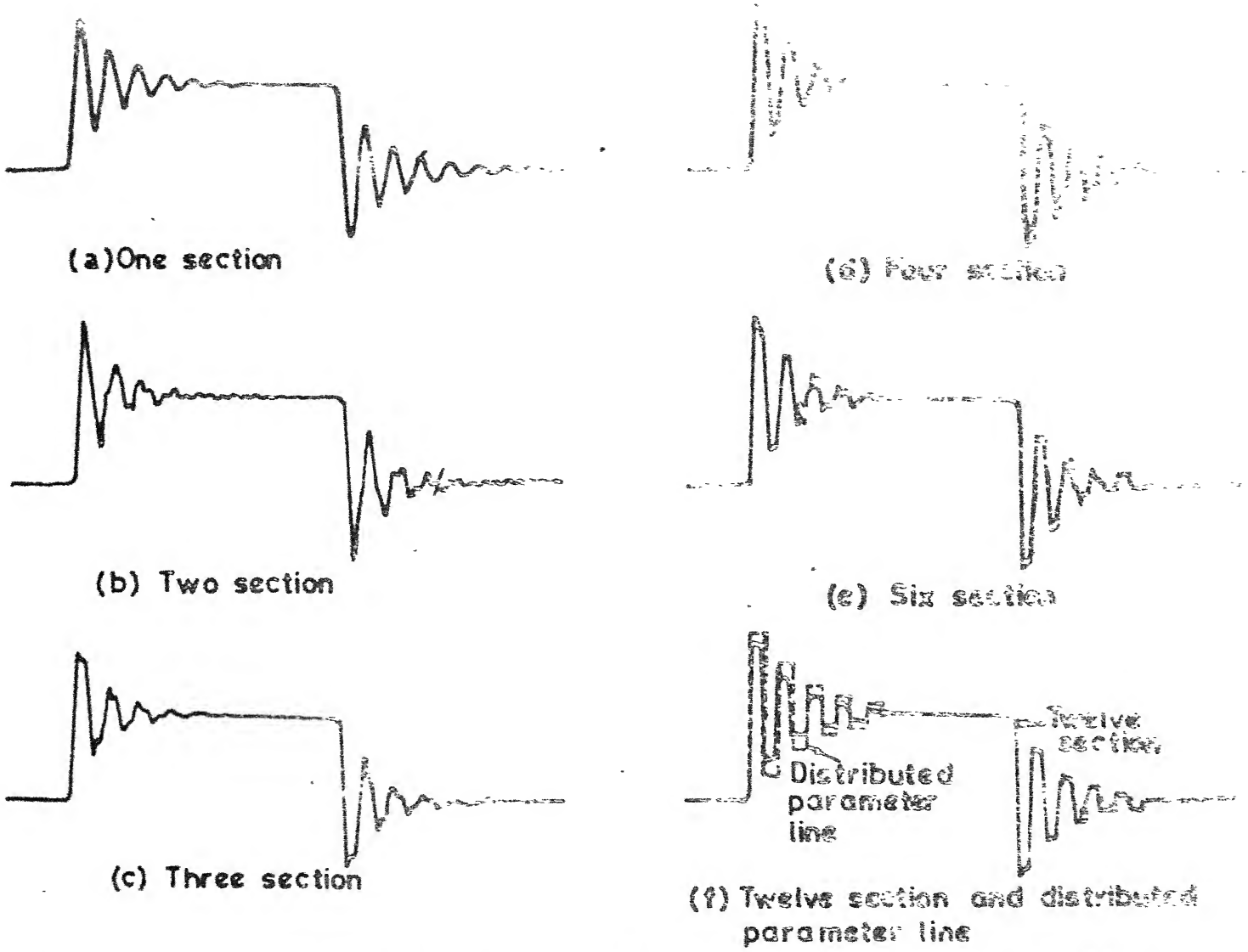

FIG. 2.1 STEP RESPONSE OF LADDER NETWORK WITH DIFFERENT NUMBER OF PI-SECTIONS

with almost simultaneous closing of the circuit breaker at the other end to connect two sections of the system together. This may occur after a line has been removed from service for maintenance or due to local disturbances caused by faults, overloading, instability or false tripping. Energization and re-energization will create a transient on the transmission line at the breaker which will propagate at nearly the velocity of light to the open end. Prior to the time the receiving end breaker closes, the initial surge will be reflected at the open end leading to an overvoltage greater than the source voltage.

In this section, switching overvoltages on a three-phase unloaded 220 kV transmission line model due to line energization, have been studied on a Transient Network Analyser.

The equivalent circuit of an unloaded line without shunt reactor compensation is shown in Figure 2.2. Switching overvoltage of the line mentioned was studied without considering source impedance. All the three phases were switched on simultaneously at different instances of the voltage waveform. The receiving end voltage waveforms for 250 km line length are shown in Figure 2.4(a). The maximum overvoltage on a phase was found to occur when it was switched on at its peak. The maximum overvoltages recorded on 250 km and 100 km lines were 1.92 p.u and 1.83 p.u respectively. Variations in the voltage waveforms as shown in the Figure 2.4(a) before they settle down to a recognizable sinusoidal pattern, are

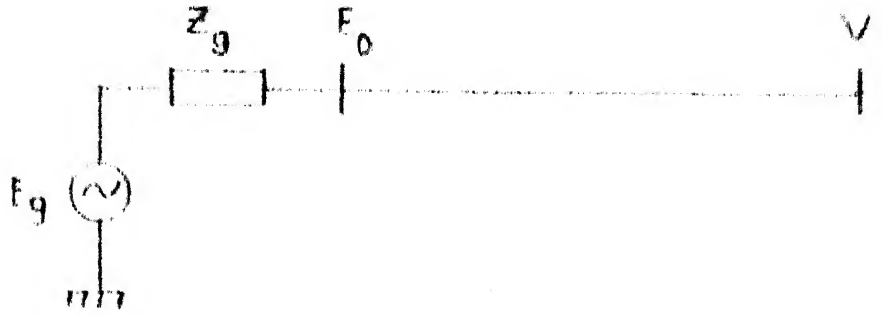

Fig. 2.2 Equivalent circuit of an unloaded line without shunt compensation.

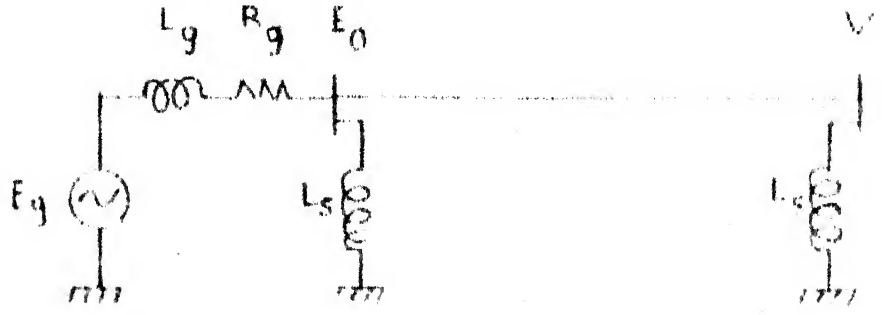

Fig. 2.3 Equivalent circuit of the unloaded line with shunt compensation.

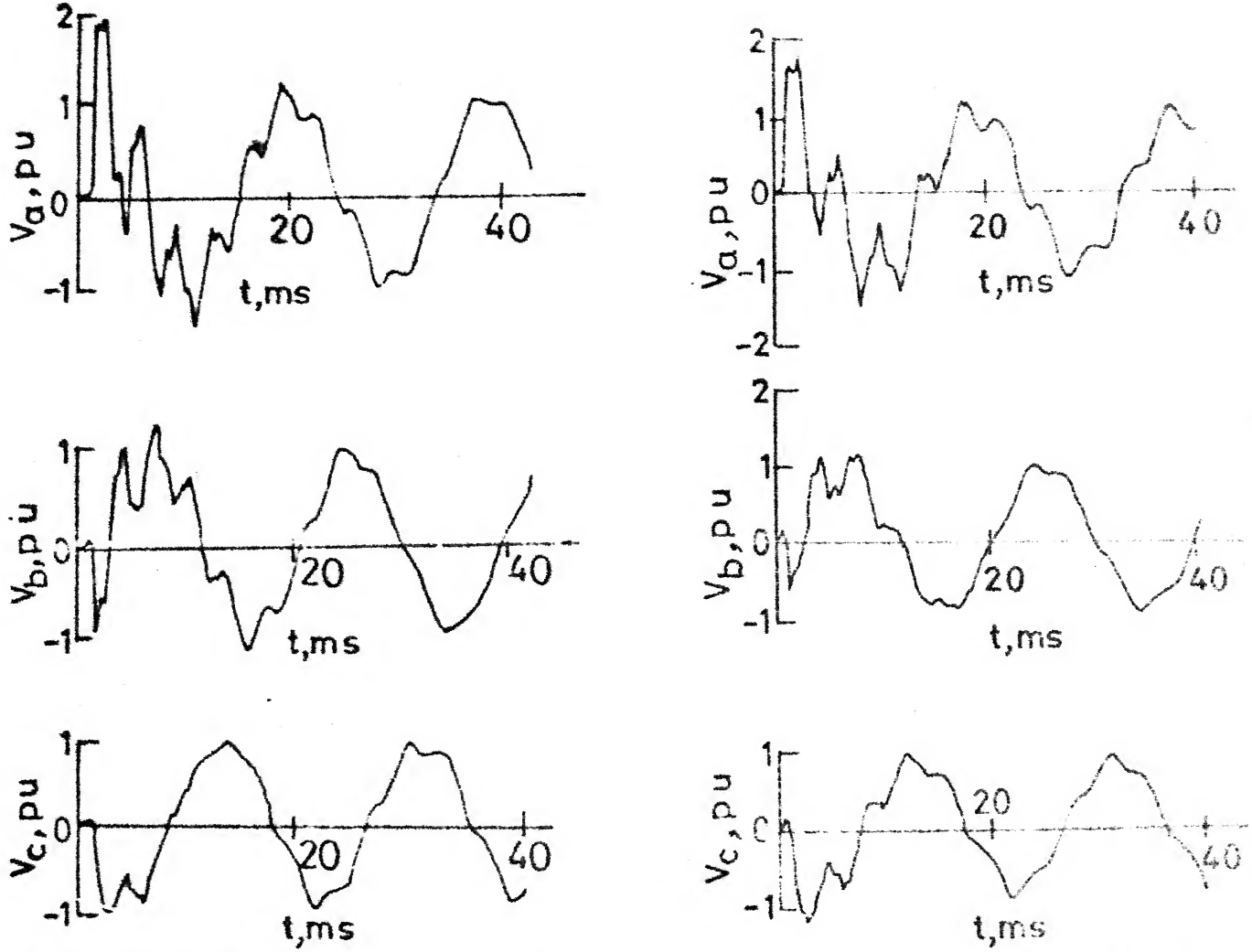

(a) Without source impedence (b) With source impedence

FIG. 2.4 RECEIVING END VOLTAGES OF 220 kV, 250 km UNLOADED LINE

found to be quite erratic. This is because of the severe reflections from the receiving end which is open.

2.4.1 Effect of source impedance:

The receiving end voltage waveforms with source impedance considered for 220 kV, 250 km line have been shown in Figure 2.4(b). The data of source impedance has been given in Appendix-E. The maximum overvoltage occurring in this case is 1.85 p.u which is less than the case when the source impedance was not considered. This is because, the source impedance normally attenuates the reflections of travelling waves and thus smoothens the transient response.

The source impedance behind the transmission line varies as the number of generator units and other equipments in operation which are added to the system, consequently changing the short-circuit power at a particular bus. So the variations in the switching overvoltage for different short-circuit powers, were observed. The following test results were obtained for a 250 km length line on TNA.

Short circuit power in MVA	Intinite	5000	2000	1000
Overvoltage in p.u.	1.92	1.86	1.80	1.78

Figure 2.5 shows the receiving end voltage waveforms of phase 'a' for different short-circuit powers as shown above.

2.4.2 Effect of line length:

The line length has a pronounced influence on switching overvoltage [9]. The effect of line lengths on switching

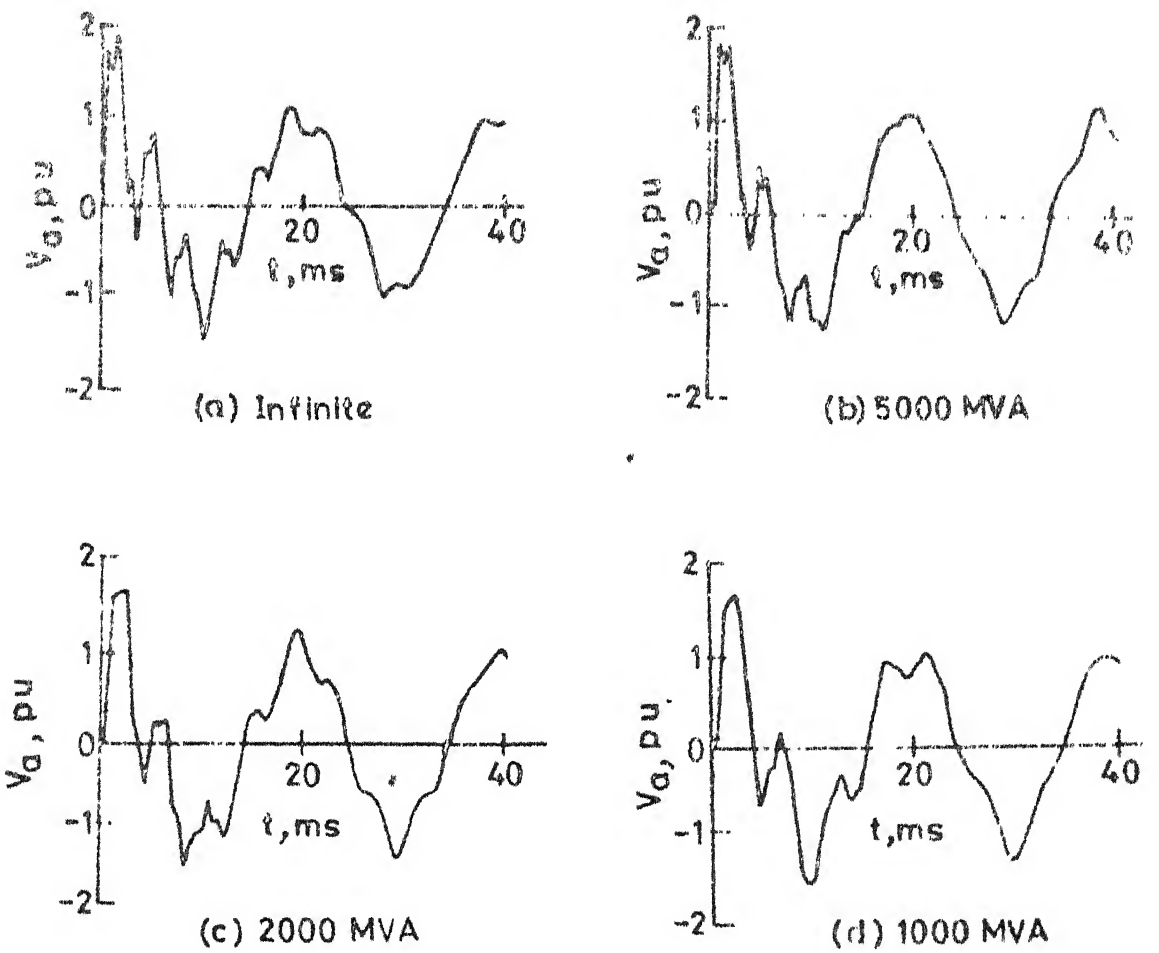

FIG. 2.5 RECEIVING END VOLTAGES OF 220 KV, 250 Km LINE FOR VARIOUS SHORT CIRCUIT POWER

overvoltages were observed for uncompensated lines of lengths 100, 250 and 350 km on the TNA. All three phases were switched on synchronously. The voltage waveforms obtained for different line lengths have been shown in Figure 2.6. From these graphs it is observed that as the line length increases, switching overvoltage also increases. The following results were observed when the switching was done with phase 'a' at its positive peaks.

Line length in km	100	250	350
Overvoltage in p.u.	1.78	1.90	2.0

2.4.3 Shunt reactor compensation:

Shunt reactors are provided at the sending and receiving ends of a transmission line to compensate for the reactive power generation of the line. This prevents excessive voltage at the receiving end of the line and the flow of leading currents through the HV systems. The equivalent circuit of an unloaded shunt compensated line is shown in Figure 2.3. On a TNA, shunt reactor are represented by an equivalent inductance L_s which depends on the size of the reactor. The degree of compensation provided by the shunt reactor is expressed as percentage of the charging power of a line. With the increase in the percentage of compensation, switching overvoltage was found to decrease. Switching overvoltages for various levels of compensation for 220 kV line of 250 km length are given below:

Percentage of compensation	0	90	100
Overvoltage in p.u.	1.86	1.81	1.78

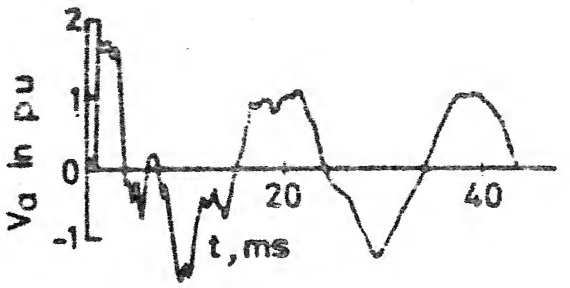

(a) 350 km

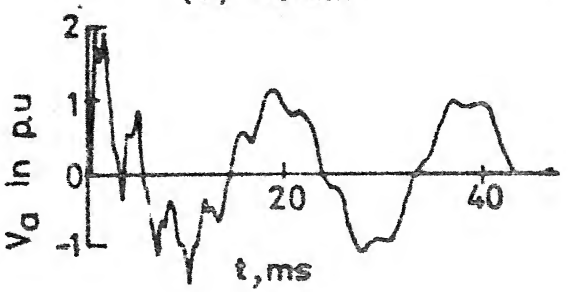

(b) 250 km

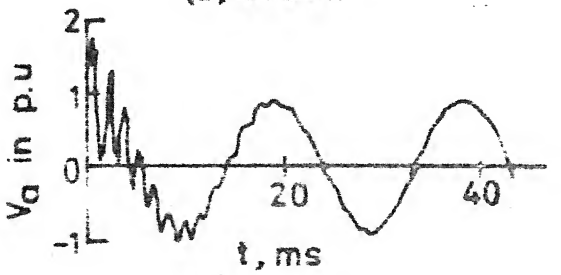

(c) 100 km

FIG 2.6 RECEIVING END VOLTAGES OF 220 kV, 250 km OPEN ENDED LINE FOR VARIOUS LINE LENGTH

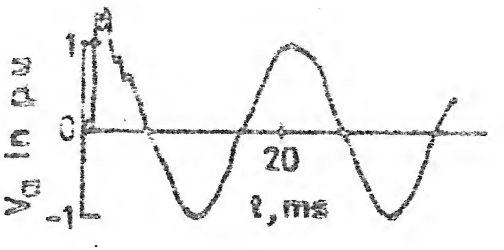

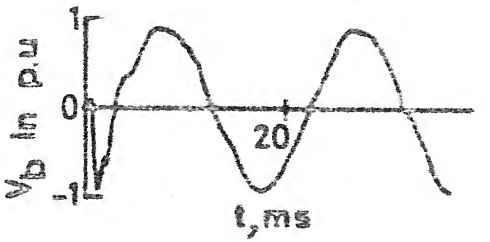

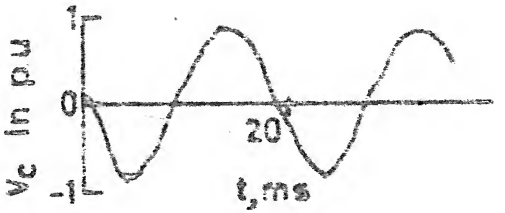

FIG. 2.7 RECEIVING END VOLTAGES OF 220 kV, 250 km RESISTIVE LOAD TERMINATED LINE. R=96.8 OHM/PHASE

2.5 Overvoltage on Resistive-Load Terminated Lines:

In this section, TNA experimentation results for switching overvoltages of lines terminated with resistive loads are described. The equivalent circuit of a resistive-load terminated line is of the form shown in Figure 2.8. The effect of source impedance and load have been investigated. The load has been represented by an equivalent resistance R whose value depends upon the amount of loading.

The overvoltage for different resistive load terminations of the line are given in Table 3.

Table 3

Switching overvoltages on resistive-load terminated lines

Line length km	Load resistance	Overvoltage in p.u.	Remarks
250	928	1.45	Without source impedance
	928	1.37	With source impedance
	400	1.00	
	242	0.99	
100	928	1.34	
	400	1.01	

The resistive load was varied from 50 MW to 200 MW for a 220 kV system and the maximum switching overvoltage observed was 1.45 p.u. at 50 MW load without considering source impedance. However with the inclusion of source impedance for

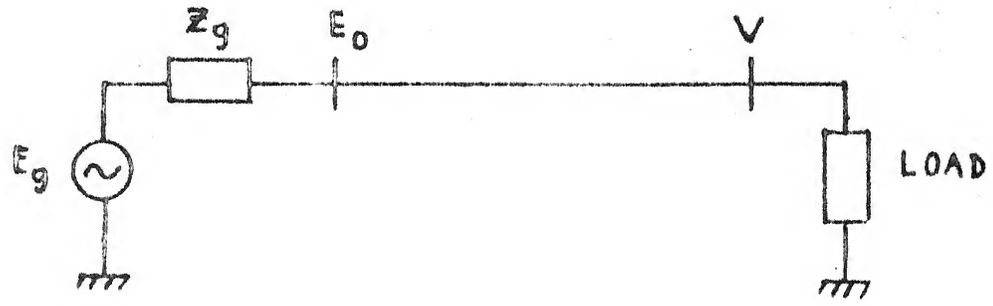

Fig. 2.8 Equivalent circuit of a line with load.

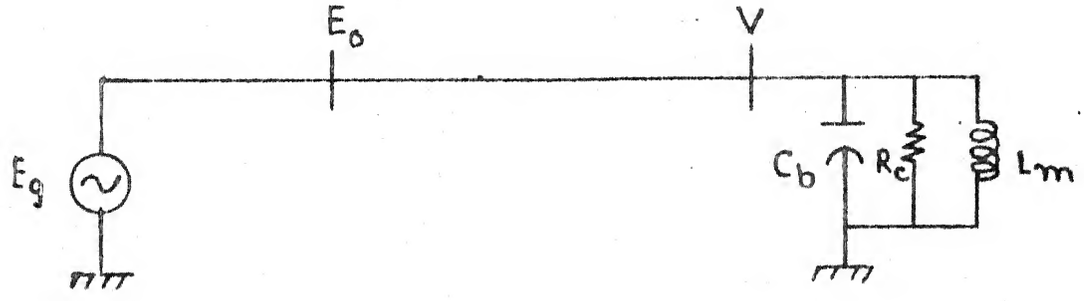

Fig. 2.9 Single line diagram of a R-L-C terminated line.

the same load, the overvoltage reduced to 1.37 p.u. The data of source impedance has been given in Appendix-E. It was also observed that switching overvoltage reduced nearly to 1.0 p.u. when the line was terminated with a resistive load nearly equal to surge impedance of the line. However the switching overvoltage increased with the increase in load resistance beyond surge impedance value. The receiving end voltage waveforms for resistive-load of 928 ohm with source impedance taken into consideration are shown in Figure 2.7.

2.6 Overvoltage on Inductive-Load Terminated Lines:

In the previous section, the switching overvoltages on resistive-load terminated lines were observed. However, in practice the loads are of lagging power factor in nature. Such loads are represented by equivalent resistance R and inductance L whose values depend upon the amount of loading and power factor. The power factor used for this study is 0.8.

The switching overvoltages for different inductive loads were observed on the TNA for different line lengths and have been summarised in Table 4 for synchronous switching with phase 'a' at its peak. The source impedance has been taken into account in this study.

The receiving end voltage waveforms for 250 km line terminated with 50 MW load are shown in Figure 2.10. It is observed that switching overvoltage for inductive load terminations are lower compared to that of an unloaded line. This is because the lagging load current serves to neutralise

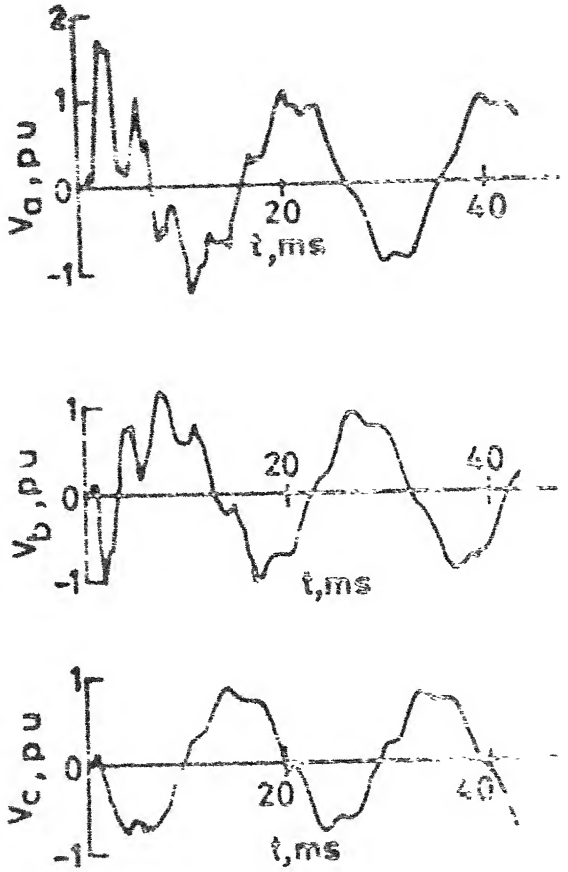

FIG 2.10 RECEIVING END VOLTAGES OF 220 kV, 250 km LINE WITH INDUCTIVE LOAD TERMINATION R=618 Ω, L = .48 H

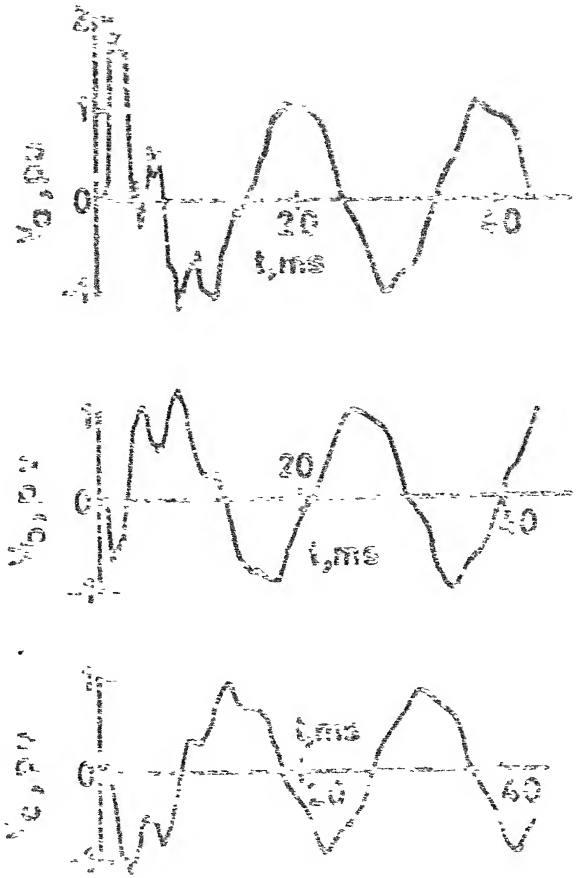

FIG. 2.11 RECEIVING END VOLTAGES OF 220 kV, 250 km LINE WITH R-L-C TERMINATION, R_c = 4.84 KΩ, L_m=15.41 H, C_b=2500 PF

Table 4

Switching overvoltage with inductive-load terminated lines

Line length, km	Load		Overvoltage in p.u.	Remarks
	R (ohm)	L (Henry)		
100	618	1.48	1.71	Load is represented by equivalent resistance and inductance
	154	0.37	1.34	
250	618	1.48	1.69	
	154	0.37	1.33	

the leading line charging current resulting in the decrease of the terminal voltage.

A comparison between the switching overvoltages with lagging power factor load and with purely resistive load of the same magnitude shows that the overvoltage is more in the case of inductive load termination.

2.7 Overvoltage on Transformer Terminated Line:

When a transmission line is switched at the sending end with a transformer connected at the receiving end, the line has a path through the magnetizing impedance of the transformer, by which it can discharge. But as long as the transformer core is unsaturated, this represents a high impedance and the discharge is therefore very slow, causing a sharp increase in voltage across the terminals of the transformer [2]. The transformer also helps to drain the

The phase to neutral switching overvoltages for the transformer terminated lines have been observed for various line lengths, transformer winding connections and different level of excitation current of the transformer.

In this study, three single-phase transformers are connected to form a three-phase bank. Variations in the level of excitation current were obtained by varying the system operating voltage. The values of 0.65 percent and 1.45 percent excitation, for which the overvoltages have been found, are on the linear portion of the magnetization characteristics while, 2.6 percent and 15.0 percent excitation is on the non-linear portion.

The results obtained when the three-phase voltages are switched simultaneously with phase 'a' at its positive peak have been given in Table 5.

The receiving end voltage waveforms of 250 km line for Star-Delta and Delta-Star connections of the transformer windings are shown in Figures 2.12(a) and 2.12(b) respectively.

From the results given in Table 5, it can be seen that for a line of given length, switching overvoltage is higher for a Star-Delta connected transformer as compared with that for a Delta-Star connection. Also, it is found that the rise in the overvoltage decreases as the level of excitation is increased.

2.8 Overvoltage on R-L-C Terminated Lines:

The effect of transformer MVA ratings on the switching overvoltage was also studied on TNA by connecting

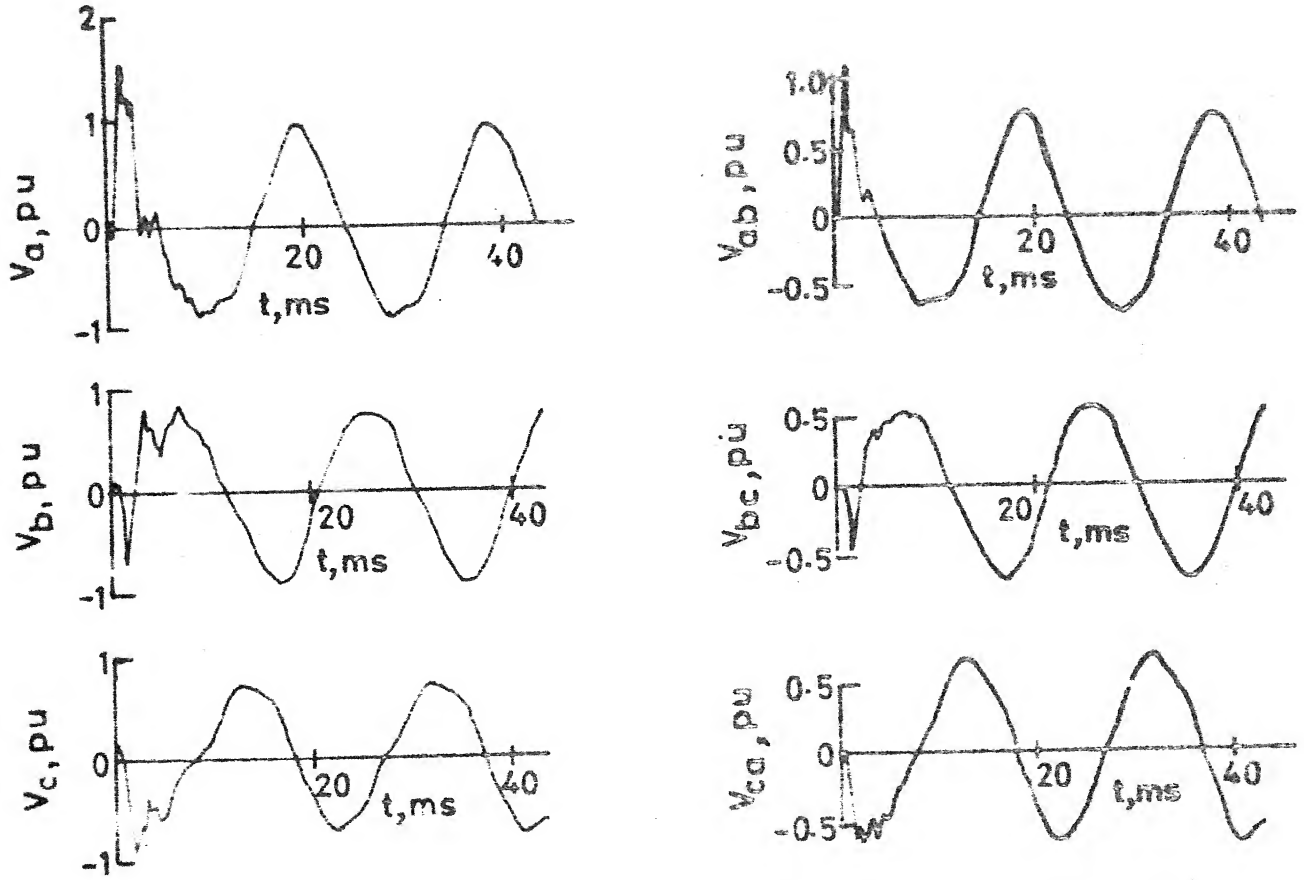

(a) Transformer connection: Star-Delta

(b) Transformer connection: Delta-Star

FIG 2.12 RECEIVING END VOLTAGES OF TRANSFORMER TERMINATED LINE PERCENTAGE OF EXCITATION - 2.6 %

Table 5

Switching overvoltages of transformer terminated lines

Line length, km	Transformer connection	Percentage of excitation	Overvoltage in p.u.
250	Star-Delta	0.65	1.38
		1.45	1.54
		2.60	1.555
		15.00	1.565
250	Delta-Star	0.65	0.987
		1.45	1.091
		2.60	1.111
		15.00	1.128
100	Star-Delta	0.65	1.44
		1.45	1.561
		2.60	1.57
		15.00	1.59
100	Delta-Star	0.65	0.88
		1.45	1.02
		2.60	1.08
		15.00	1.11

several combinations of resistance, inductance and capacitance at the receiving end of the line. The transformer is represented by its magnetising inductance, core loss resistance and bushing capacitance [14]. The single line diagram of the system studied is shown in Figure 2.9 where,

C_b : bushing capacitance

L_m : magnetizing inductance of the transformer

R_c : core loss resistance.

The inductance L_m is calculated by assuming that no load current of the transformer is 5% of its full load value. Experimental results of switching overvoltage of 220 kV line for different transformer ratings for synchronous switching are tabulated in Table 6.

Table 6

Phase to neutral overvoltages with R-L-C terminations

Line length (km)	R_c (ohm)	L_m (H)	C_b (pF)	Overvoltage in p.u.	Rating of the transformer in MVA
250	2402	6.71	2500	1.80	400
	4032	12.82	2500	1.805	240
	6452	20.55	2500	1.81	150
	9680	30.83	2500	1.82	100
100	2402	6.71	2500	1.82	400
	9680	30.83	2500	1.845	100

The receiving end voltage waveforms for 220 kV, 250 km line terminated with R = 4032 ohm, L_m = 12.82 H and C_b = 2500 pF (an equivalent of 240 MVA transformer) are shown in Figure 2.11.

From the experimental results it is found that with the increase in the MVA ratings of transformer, the magnitude of switching overvoltage decreases.

CHAPTER 3

DIGITAL CALCULATION OF PHASE TO NEUTRAL SWITCHING OVERVOLTAGE

3.1 Introduction:

Digital computer are employed for the calculation of transient phenomena on power system networks caused by switching operation, because, it does have the ability to process a vast amount of data in a systematic way, and do so in an extremely short time.

In this chapter, phase to neutral switching overvoltage for three phase distributed parameter lines are calculated using a generalised digital computer program developed. The system conditions which have been considered in the above program are; the unloaded line, resistive-load terminated line, inductive-load terminated line and transformer terminated line. The effect of source impedance, simultaneous and non-simultaneous closure of circuit breakers and the case of failure of a circuit breaker to close have also been taken into account. Switching surge control by using shunt reactor compensation and pre-insertion resistor have also been studied.

The switching overvoltage calculation have been performed by Uram and Miller method [3, 4] for 220 kV and 400 kV lines. Details of these lines are given in Appendix-E. The results of digital calculation for the 220 kV line are compared with the results obtained from the Transient Network Analyser.

3.2 Outline of the Method:

The equivalent circuit for a section of a three phase distributed parameter line, used by Uram and Miller [3, 4] for deriving the transmission line voltage and currents equations are given in Figure 3.1.

In this method, in the first step, partial differential equations governing the currents and voltages are developed from the equivalent circuit of the transmission line. The partial differential equations are then reduced to ordinary differential equations by using Laplace transformation. These differential equations are solved through a transformation of co-ordinates, which produces a general solution for the system voltage and currents. By using the appropriate boundary conditions, at the sending and receiving ends of the line, the particular solution of the three-phase transmission line is calculated numerically through the unique application of time-delay function with a digital computer program.

The general expression for current and voltages at the sending and receiving ends of the line are derived in Appendix-F. The expressions for the sending end voltages and currents are given by the equations as following:

$$[E_o(t)] = [T][k_1(t)] + [T][k_2(t)] \quad (3.1)$$

$$[I_o(t)] = [T][Z]^{-1}[k_1(t)] - [T][Z]^{-1}[k_2(t)] \quad (3.2)$$

while those of receiving end voltages and currents are:

$$[V(t)] = [T][a_1(t)] + [T][b_2(t)] \quad (3.3)$$

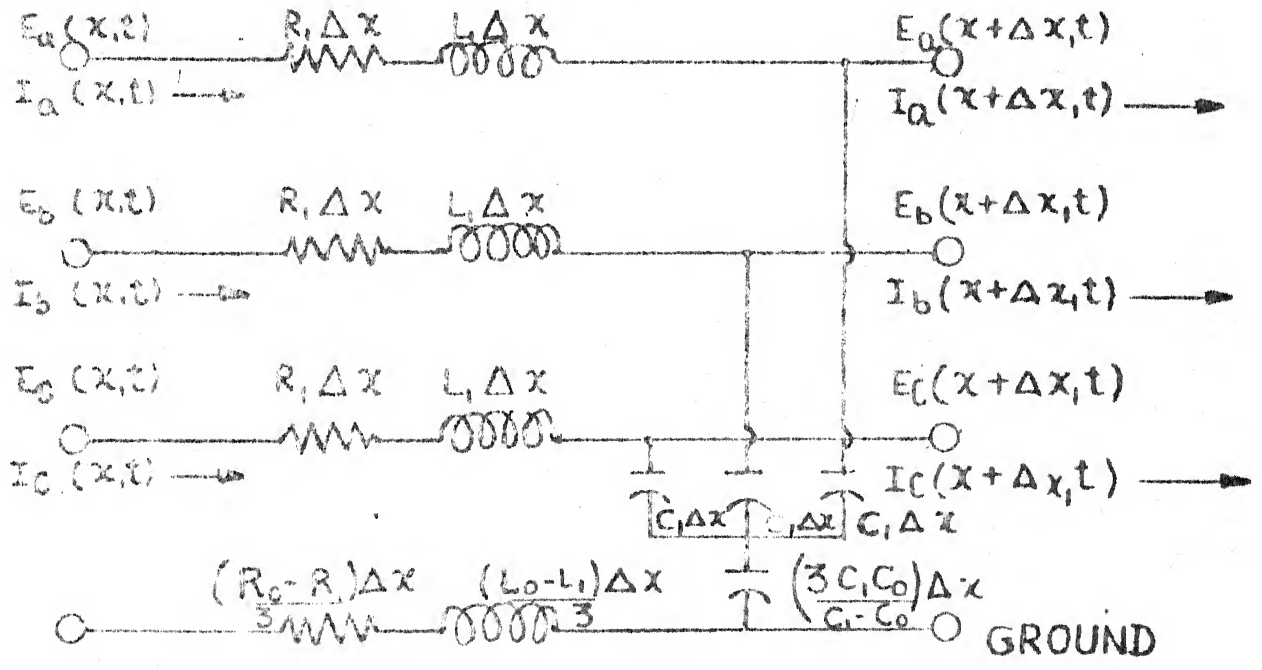

FIG. 3.1 EQUIVALENT CIRCUIT FOR 3-PHASE TRANSMISSION LINE

$$[I_1(t)] = [T][Z]^{-1}[a_1(t)] - [T][Z]^{-1}[b_2(t)] \qquad (3.4)$$

where $[Z]$ = surge impedance matrix

$[T]$ = transformation matrix

and $[a_1(t)]$, $[b_2(t)]$, $[k_1(t)]$ and $[k_2(t)]$ are matrices containing constants and they are related in Appendix-F as given below:

$$[a_1(t)] = [\alpha][k_1(t - T')\ U\ (t - T')] \qquad (3.5)$$

$$[k_2(t)] = [\alpha][b_2(t - T')\ U\ (t - T')] \qquad (3.6)$$

where T' is called the delay factor and $[\alpha]$ is the attenuation factor matrix. In equations (3.5) and (3.6), the functions

$$\begin{aligned} a_1(t) &= 0, \quad \text{for } t \leq T' \\ k_2(t) &= 0, \quad \text{for } t \leq T' \end{aligned} \qquad (3.7)$$

From equations (3.1) and (3.4), we get

$$[k_1(t)] = [T]^{-1}[E_o(t)] - [k_2(t)] \qquad (3.8)$$

$$[b_2(t)] = [a_1(t)] - [Z][T]^{-1}[I_1(t)] \qquad (3.9)$$

The calculations of unknown quantities have been done on incremental basis using the advantage of delay factor and the system boundary conditions at the sending and receiving ends of the line. In general, the main steps that are followed in incremental solution of transmission line voltages and currents are:

1. Delay factor T' is found.

2. A proper choice of time interval Δt, is made. All computations are started at t = 0.
3. The delay matrices $[a_1(t)]$ and $[k_2(t)]$ are evaluated from equations (3.5) and (3.6) respectively.
4. The matrices $[b_2(t)]$ and $[k_1(t)]$ are computed from the known boundary conditions at the sending and receiving end of the line derived in Appendix-G.
5. Matrices $[b_2(t)]$ and $[k_1(t)]$ are stored for future computation of matrices $[a_1(t)]$ and $[k_2(t)]$.
6. The unknown voltage and currents are calculated.
7. The time t is then increased by Δt and computations are repeated from step 3 onwards.

3.3 Unloaded Line without Source Impedance:

This system condition is simulated by a voltage source at the sending end of the transmission line having no source impedance and by keeping the receiving end open. The corresponding equivalent circuit is shown in Figure 3.2. The matrices $[k_1(t)]$ and $[b_2(t)]$ are derived based upon the knowledge of system boundary conditions. These derivations have been given in Appendix-G. The final expressions for $[k_1(t)]$ and $[b_2(t)]$ are as following:

$$[k_1(t)] = [T]^{-1}[E_g(t)] - [k_2(t)] \qquad (3.10)$$

$$[b_2(t)] = [a_1(t)] \qquad (3.11)$$

For the 220 kV, 250 km line and the 400 kV line whose details are given in Appendix-E, the receiving end voltages have been calculated based on the algorithm described in

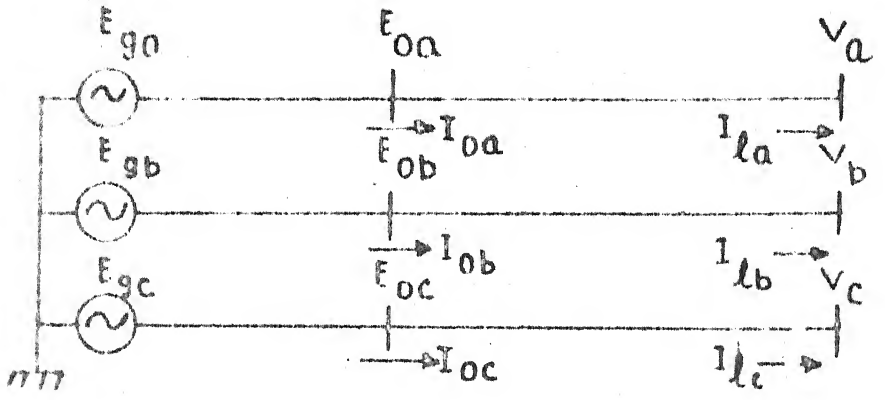

Fig. 3.2 Three phase unloaded line without source impedance.

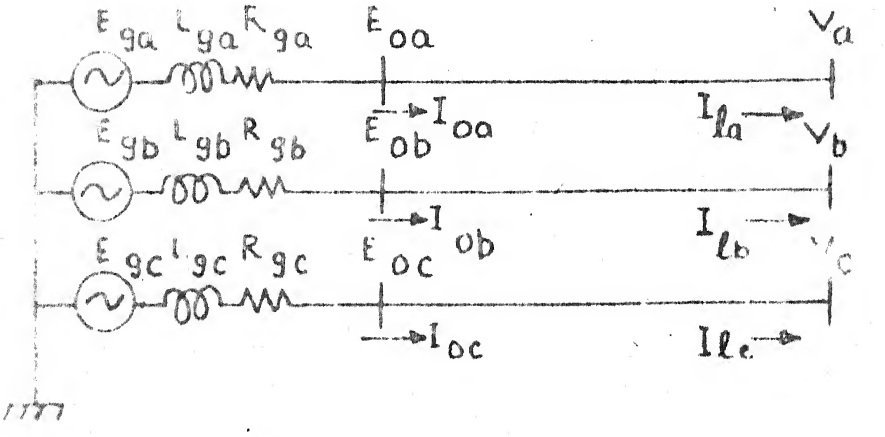

Fig. 3.3 Three phase unloaded line with source impedance.

the previous section. The time interval used in the digital calculation is 55 microsec. The receiving end voltage waveforms for a 400 kV line for simultaneous closure of circuit breakers are shown in Figure 3.4. In the above figure the duration of transients are observed to be quite long. This is due to the absence of load current which would otherwise serve to damp the oscillations. The maximum overvoltage is found to be 1.95 p.u., when phase 'a' is switched at its peak. By comparing the voltage waveforms of phase 'a' in Figures 3.4(a) and 3.4(b), it has been observed that the transient in Figure 3.4(b) is more irregular compared to Figure 3.4(a). This is because in the first case the sending end voltage of phase 'a' is passing through zero magnitude at the instant of switching while in second case a finite magnitude of the voltage is present at that instant. The voltage waveforms for 220 kV, 250 km long line is shown in Figure 3.5(a) and the maximum overvoltage which is found to be 1.93 p.u. is in close agreement with result obtained on TNA.

The switching overvoltages of 400 kV line are calculated for non-simultaneous closure of circuit breakers when the three phases are switched at their positive peaks in the sequence a-b-c. The maximum overvoltage that occurred was 2.34 p.u. as shown in Figure 3.5(b). The time delay of non-simultaneous switching is simulated on the digital computer by inserting a high resistance value of 10^{10} ohm in series with the source voltage.

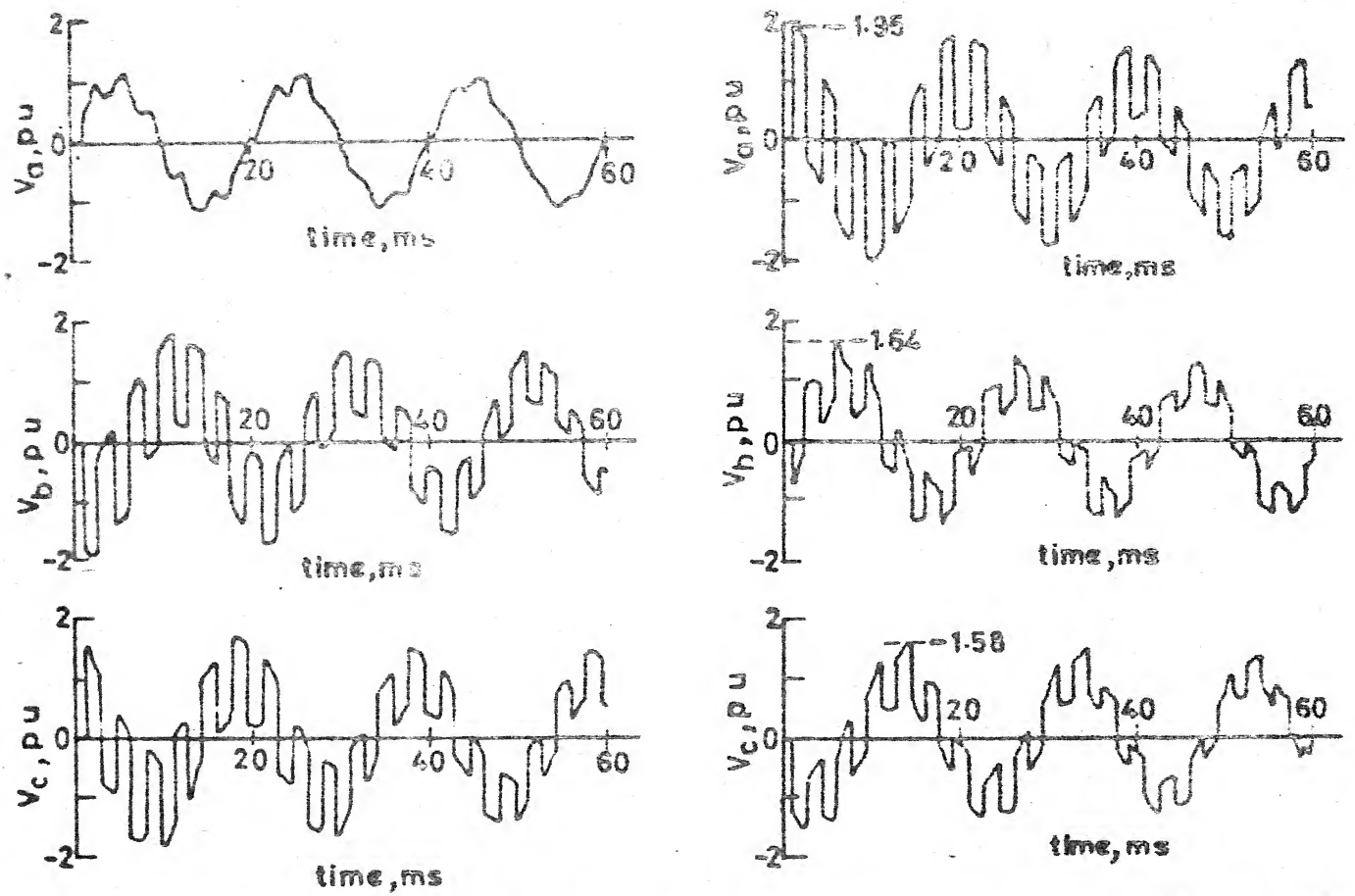

(a) Angle of switching : 0°,-120°&120° of phases a,b & c respectively

(b) Angle of switching : 90°,-30° & 210° of phases a,b & c respectively

FIG. 3.4 • RECEIVING END VOLTAGES OF 400 kV, 230 km UNLOADED LINE WITHOUT SOURCE IMPEDENCE

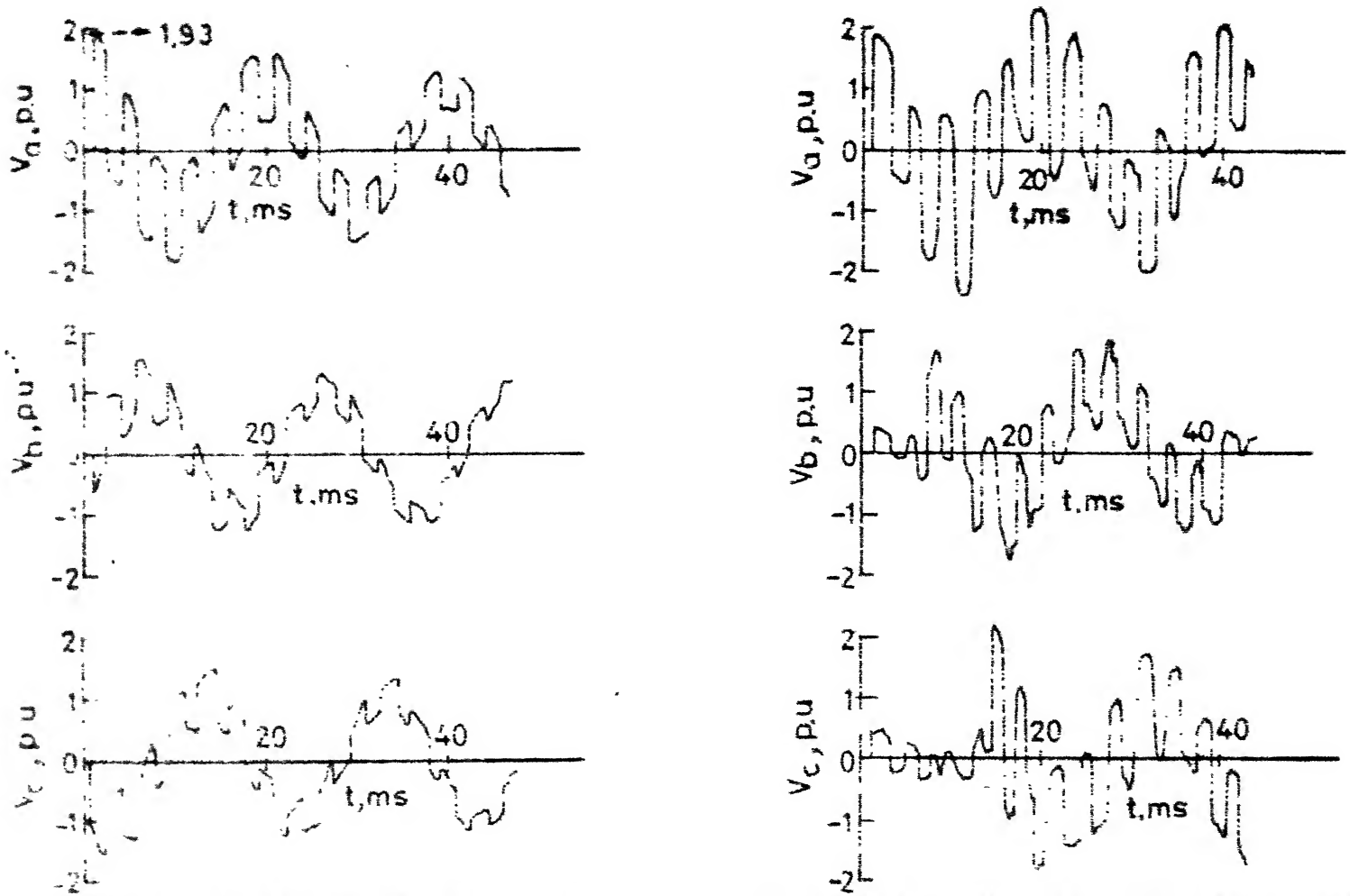

(a) 230kV, 250 km line. Angle of Switching: 90° -30° & 210°

(b) 400 kV, 230 km line. Three phases are switched at their positive peaks

FIG 3.5 RECEIVING END VOLTAGES OF UNLOADED LINE WITHOUT SOURCE IMPEDANCE

3.4 Unloaded Line with Source Impedance:

With the inclusion of source impedance, a decrease in switching overvoltage is reported by several authors [9, 11]. Therefore, in this section the effect of source impedance has been taken into account in finding out the switching overvoltages. The equivalent circuit of the system studied is shown in Figure 3.3. The known boundary conditions are the currents at the receiving ends and source voltages at each phase. Since the boundary conditions at the receiving end are same as in Section 3.3, the expression for the matrix $[b_2(t)]$ will be of the same form as given by equation (3.11). The matrix $[k_1(t)]$ is derived as following.

$$\frac{d}{dt}[k_1(t)] = \frac{d}{dt}[k_2(t)] + [\gamma][T]^{-1}[E_g(t)] - [\gamma][W][k_1(t)] + [\gamma][X][k_2(t)] \qquad (3.12)$$

The derivation of these equations are given in Appendix-G. The differential equations in equation (3.12) are solved by utilizing Eulers predictor-corrector formula [22].

Voltage waveforms at receiving end for the 220 kV, 230 km and the 400 kV line with source impedance are shown in Figures 3.6(a) and 3.6(b) respectively. Magnitudes of source impedance, which are given in Appendix-E, have been calculated from source short circuit power. The maximum overvoltage for the 220 kV, 250 km and 400 kV lines are found to be 1.90 p.u. and 1.92 p.u. respectively. In both these cases a decrease in overvoltage is observed because of the source impedance, which attenuates the reflections of

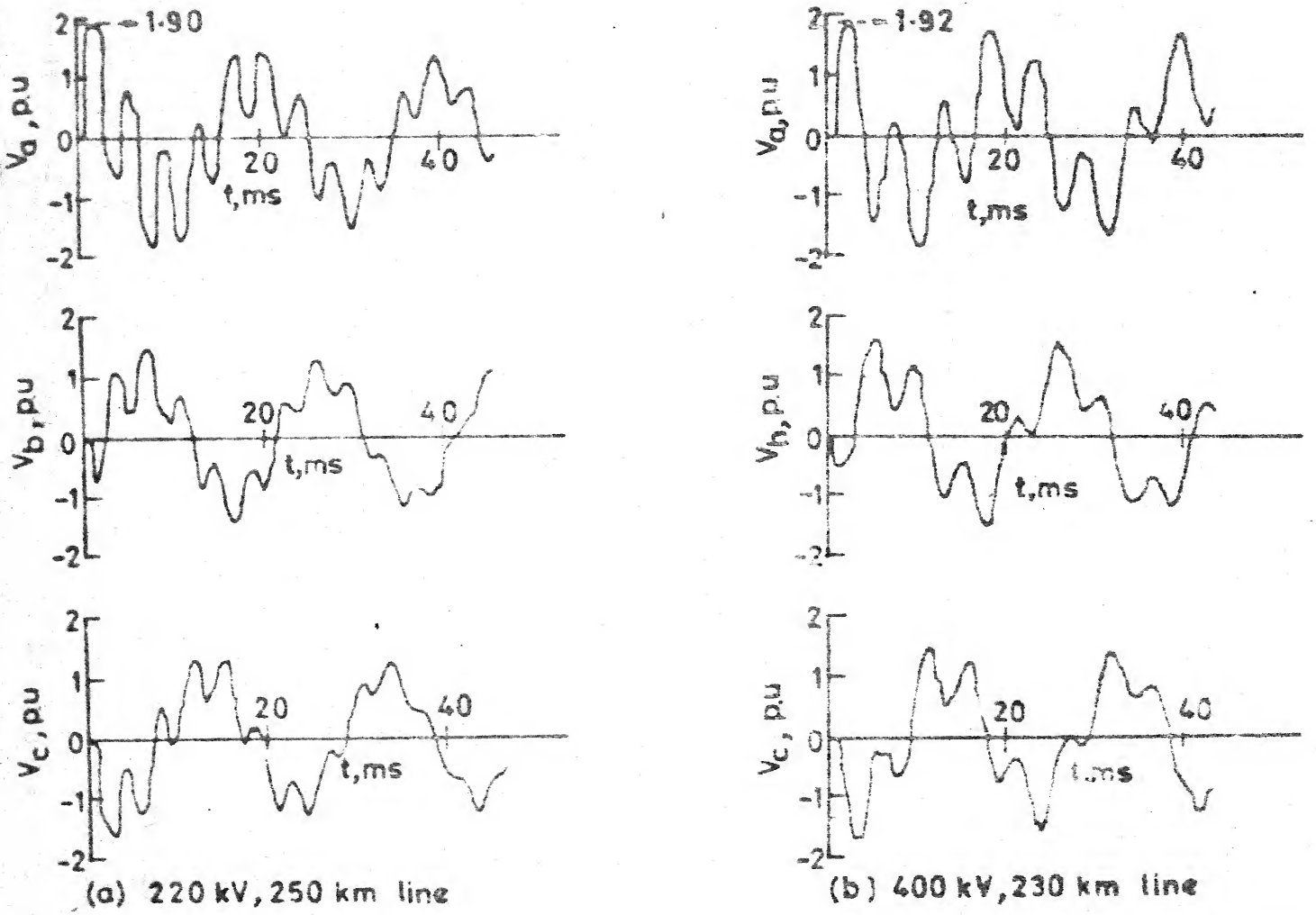

FIG 3. 6 RECEIVING END VOLTAGES OF UNLOADED LINE WITH SOURCE IMPEDANCE. ANGLE OF SWITCHING : 90°, -30° & 210°

travelling waves and thus smoothens the transient response. The result of digital calculations for the 220 kV line were compared with the results obtained from TNA and the two were found to be in close concurrence.

The switching overvoltages of unloaded line, when the sending end circuit breaker in any phase fails to close, have also been calculated. The open phase was simulated on digital computer by inserting a resistance of the value 10^{10} ohm. The receiving end voltage waveforms for the failure of the sending end breaker of phase 'a' are shown in Figure 3.7. From this figure it is seen that a small voltage appears at the receiving end of the open phase, even though the source of this phase is not connected. The maximum overvoltage is found to be 2.05 p.u.

3.5 Line with Resistive-Load Terminations:

In this section, switching overvoltages of resistive load terminated lines have been calculated. The load is represented by an equivalent resistance corresponding to the amount of loading. The switching overvoltage of a line terminated with resistive load is less severe as compared to that on an open ended line [5]. The load current reduces the severe reflections of travelling waves and hence serves to damp the oscillations. The equivalent circuit of the system studied is shown in Figure 3.9. The expression for the matrix $[k_1(t)]$ is of the form as given in equation (3.12). The matrix $[b_2(t)]$ is derived in Appendix-G by applying the boundary conditions existing

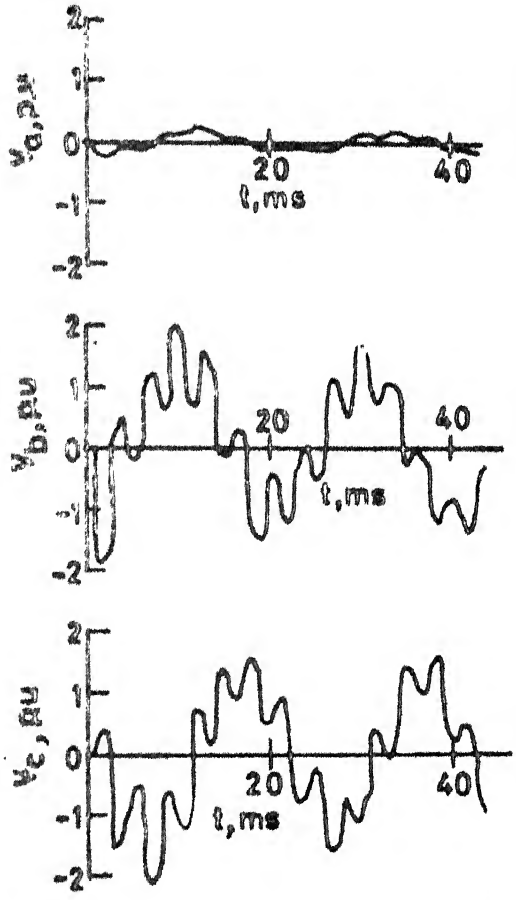

FIG. 3.7 RECEIVING END VOLTAGES OF 400 kV UNLOADED LINE WITH SENDING END BREAKER OF PHASE 'a' OPEN. ANGLE OF SWITCHING : 30°, -90° & 150°

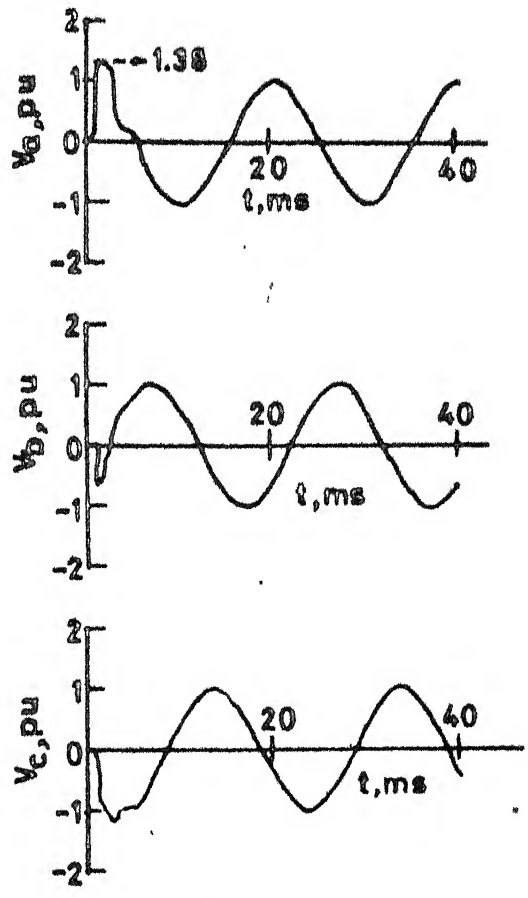

FIG. 3.8 RECEIVING END VOLTAGES OF 220 kV, 250 km LINE WIT RESISTIVE LOAD. R = 928 Ω ANGLE OF SWITCHING : 90 -30° & 210°

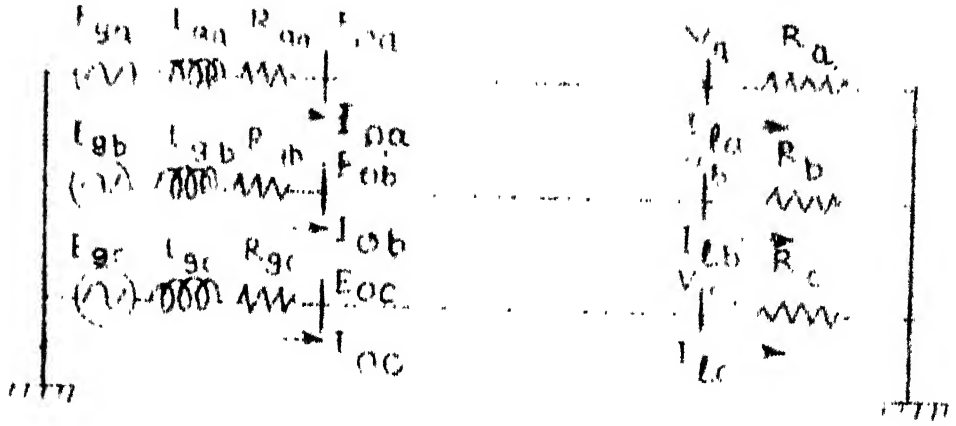

Fig. 3.9 Three phase transmission line with resistive load.

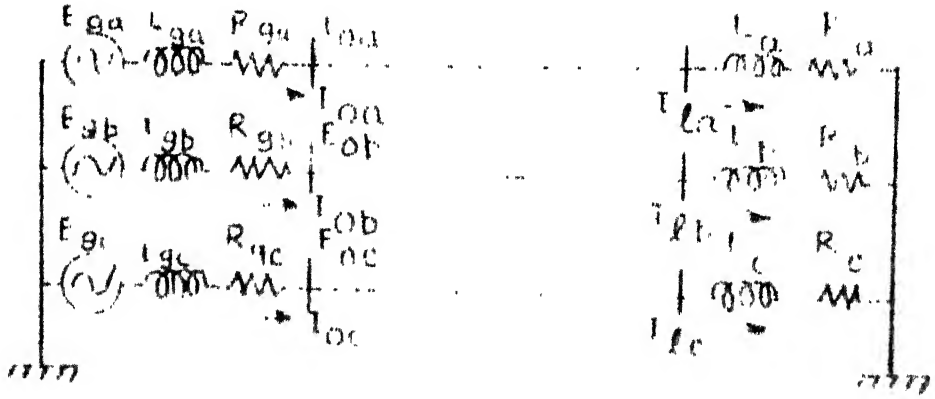

Fig. 3.10 Three phase transmission line with inductive load.

at the receiving end of the line. The solution of $[b_2(t)]$ is given as following:

$$[b_2(t)] = [[T]^{-1}[R][T][Z]^{-1} + [U]] \times [[T]^{-1}[R][T][Z]^{-1} - [U]] \quad (3.13)$$

The receiving end voltage waveforms of the 220 kV, 250 km line for a resistive-load of 928 ohm and with source impedance being taken into consideration are shown in Figure 3.8. The maximum overvoltage is found to be 1.38 p.u. which is in close proximity with the TNA results. The overvoltage of 400 kV line terminated with a load of 400 MW for the synchronous closure of the circuit breakers is found to be nearly equal to unity. The voltage waveforms for the above case are shown in Figure 3.11(a).

Figure 3.11(b) shows receiving end voltage waveforms of the 400 kV line for asynchronous closure of the breaker when the phases are switched at their respective positive peaks in the sequence a-b-c. There is no signiricant difference in the magnitude of overvoltage when compared with the case for synchronous closure of breakers.

For a 400 kV line, the switching overvoltage when a breaker at the receiving end fails to close, has also been calculated. The receiving end voltage waveforms, in case when phase 'a' circuit-breaker at the receiving end fails to close and with the phase having loads of 133 MW each, are shown in Figure 3.12. The maximum overvoltage in phase 'a' in this condition is 2.04 p.u. The overvoltages in the other two phases are found to be lower

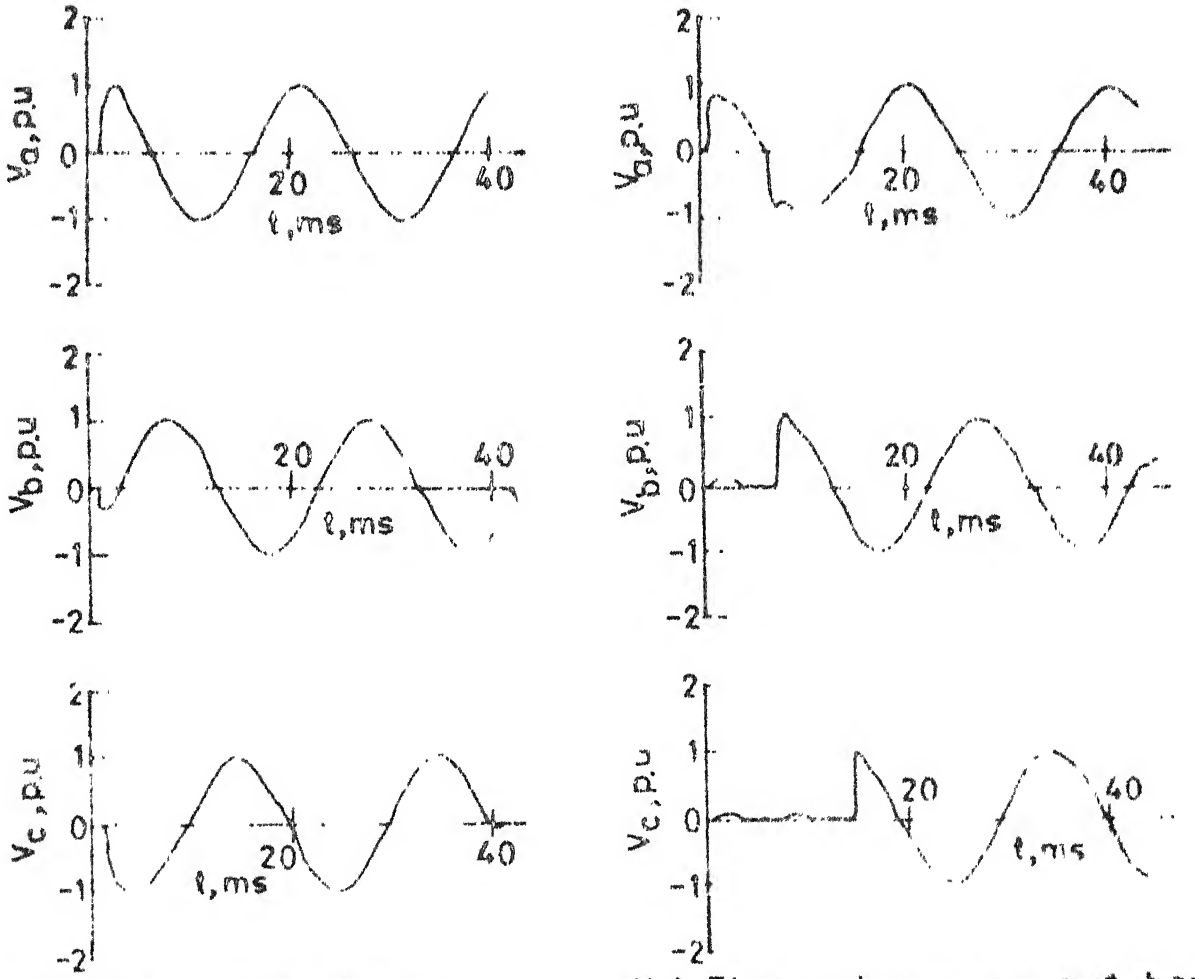

(a) Angle of switching: 90°, -30° & 210°

(b) Three phases are switched at their positive peaks

FIG 3.11 RECEIVING END VOLTAGES OF 400 kV, 230 km LINE WITH RESISTIVE LOAD TERMINATION LOAD = 400 MW

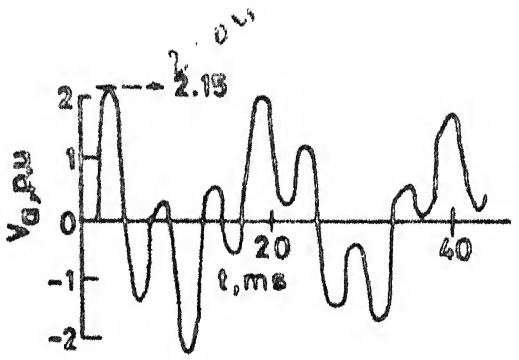

FIG.3.12 RECEIVING END VOLTAGES OF 400 kV. RESISTIVE LOAD TERMINATED LINE WITH RECEIVING END BREAKER OF PHASE 'a' OPEN. ANGLE OF SWITCHING : 90°, -30° & 120°

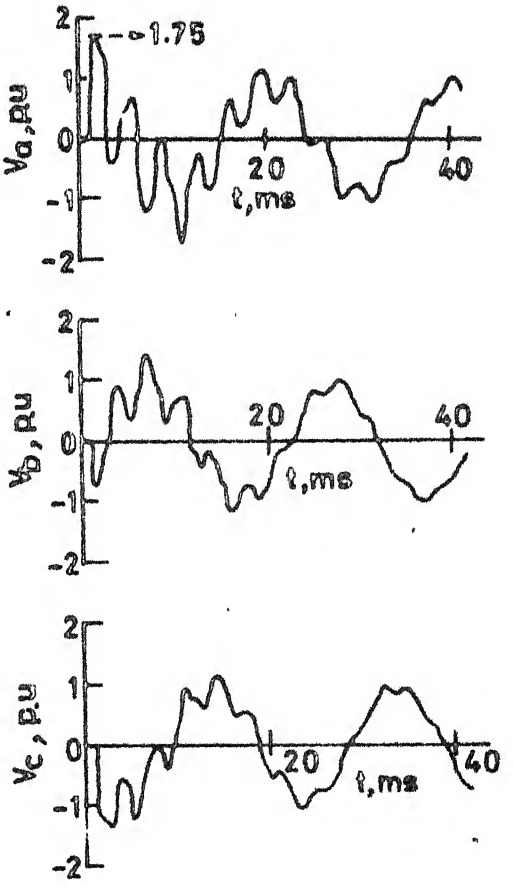

FIG. 3.13 RECEIVING END VOLTAGES OF 220 kV, 250 km INDUCTIVE LOAD TERMINATED LINE R = 618 Ω, L = 1.48H. ANGLE OF SWITCHING : 90°, -30° & 210°

compared to that in phase 'a' because the load current damps the oscillations and smoothens the voltage waveforms.

3.6 Line with Inductive Load Terminations:

In the previous section, the switching overvoltage for unity power factor loads have been calculated but in practice most of electric utility loads are of lagging power factor. The equivalent circuit of the inductive-load terminated line is shown in Figure 3.10. The load is represented by an equivalent resistance and inductance whose magnitude depends upon the amount of loading and power factor. The solution of matrix $[k_1(t)]$ is same as given in equation (3.12). Based on the boundary conditions at the receiving end of the line, the solution of matrix $[b_2(t)]$ is derived in Appendix-G and is given as follows:

$$\frac{d}{dt}[b_2(t)] = \frac{d}{dt}[a_1(t)] + [J][M][a_1(t)] - [J][N][b_2(t)] \qquad (3.14)$$

The matrices [J], [M] and [N] are defined in Appendix-G.

The receiving end voltages of the 220 kV, 250 km and the 400 kV lines for simultaneous closure of the breaker are calculated and the resulting voltage waveforms are shown in Figures 3.13 and 3.14(a) respectively. The overvoltage occurring on a 220 kV, 250 km line for a load of 50 MW with power factor 0.8 was found to be 1.75 p.u. while the value obtained using the TNA for the same load was 1.69 p.u. For the 400 kV line with a load of 400 MW, the overvoltage was found to be 1.27 p.u. for simultaneous closure of the breaker.

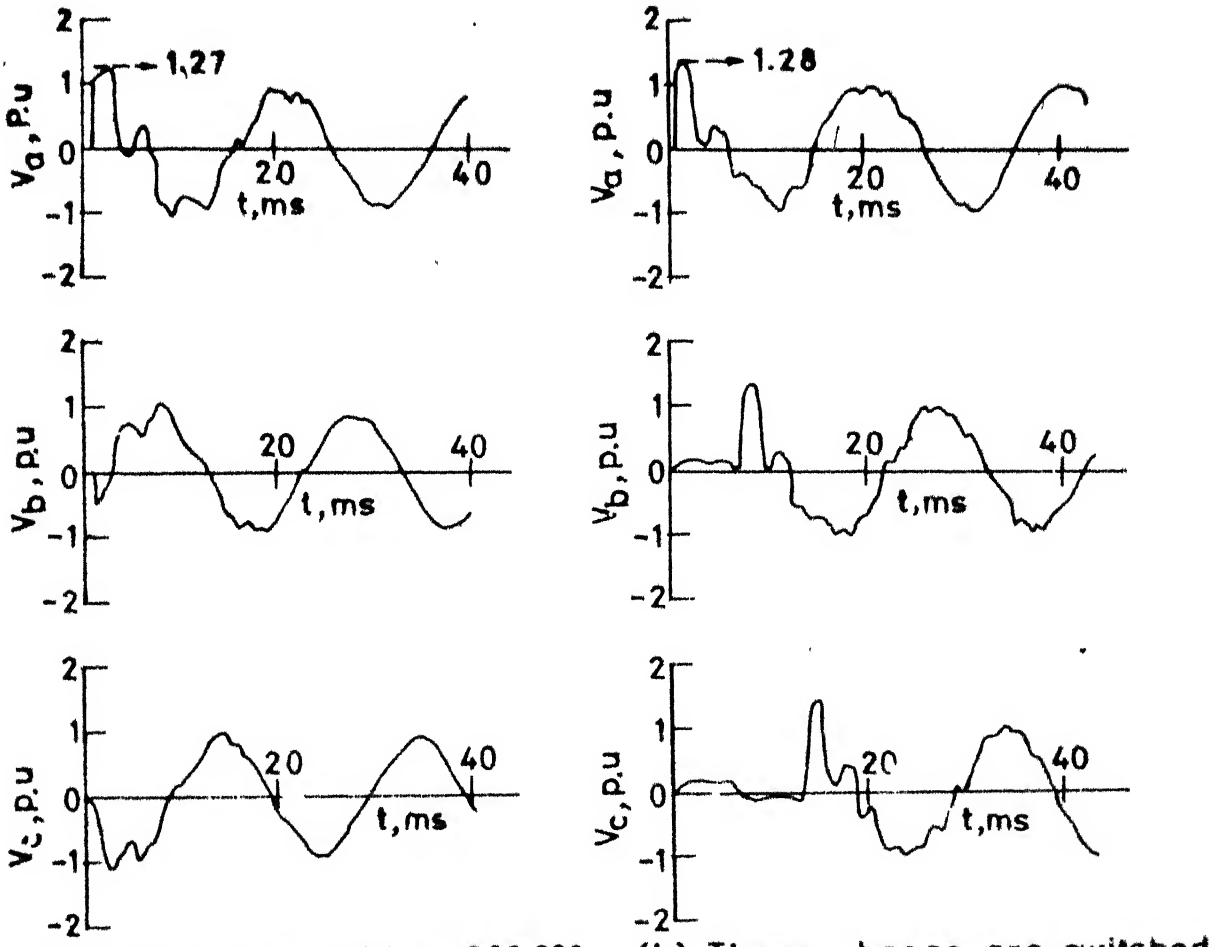

(a) Angle of switching: 90°, -30° and 210°

(b) Three phases are switched at their positive peaks

FIG 3.14 RECEIVING END VOLTAGES OF 400 kV LINE WITH INDUCTIVE LOAD TERMINATION. LOAD = 400 MW, P.F = 0.9

The receiving end voltages of the 400 kV line for non-simultaneous closure of breakers when the three phases are switched at their positive peak in the sequence a-b-c have also been calculated and the waveforms are shown in Figure 3.14(b). There is no significant difference in the magnitude of overvoltage when compared with the case of simultaneous closure of circuit breakers.

3.7 Line with Transformer Termination:

Switching overvoltages are experienced when a transmission line is terminated with unloaded transformer [2, 11, 14]. The equivalent circuit of a transformer is shown in Figure 3.15.1. Its leakage inductance is represented by L_t and the series resistance R_t accounts for the copper loss. The magnetizing inductance is represented by L_m and the core loss is represented by R_c. In calculating the switching overvoltage of a line terminated with unloaded transformer, the transformer is simulated by its magnetizing inductance L_m and resistance R_c alone since the leakage impedance of an unloaded line is extremely small. The reduced equivalent circuit of a transformer considering only the magnetizing branch is shown in Figure 3.15.2. The parallel circuit consisting of L_m and R_c can be reduced to a series equivalent circuit of L and R is shown in the above figure. The voltages at the receiving end of the transformer terminated line was calculated by following the same method as outlined in the Section 3.6 for an inductive-load terminated line with source impedance.

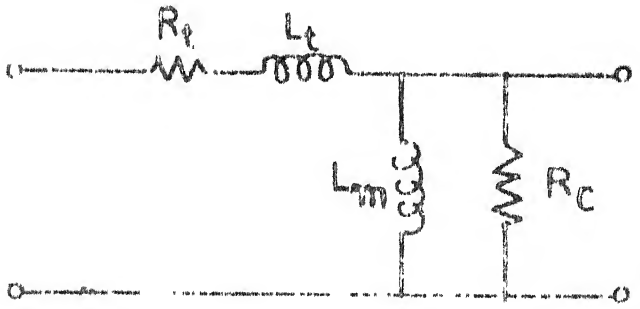

Fig. 3.15.1 Equivalent circuit of a transformer.

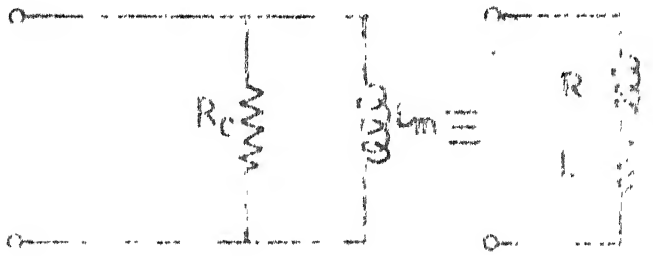

Fig. 3.15.2 Equivalent circuit to represent an unloaded transformer.

The switching overvoltages for the 400 kV line having an unloaded transformer of 480 MVA at the receiving end have been calculated and the waveforms obtained are shown in Figure 3.16(a). The maximum overvoltage is found to be 1.83 p.u.

Switching overvoltages due to faults occurring on the secondary side of the transformer have also been calculated. The transformer in this case is represented by its leakage impedance only. The numerical values of L_t and R_t used in this calculation were, L_t = 0.6 H and R_t = 5 ohm, which closely represents a 100 MVA transformer. Plots of the receiving end voltage waveforms are shown in Figure 3.16(b). The maximum overvoltage is observed to be 1.16 p.u. An increase in the size of the transformer reduces the leakage reactance and hence a decrease in switching overvoltage is expected. This was confirmed by the computation exercise.

3.8 Effect of Shunt Reactor Compensation:

The continuous increase in voltage, line lengths and number of conductor per bundle in EHV systems has emphasized the importance of the excess of line MVAR and of the associated voltage and reactive power control. The adoption of shunt reactors to compensate a portion of line charging Mvars is an indispensible method for controlling excessive voltage and leading currents flowing through the system. For the study of the switching-surge characteristics of a shunt compensated transmission line, the system illustrated

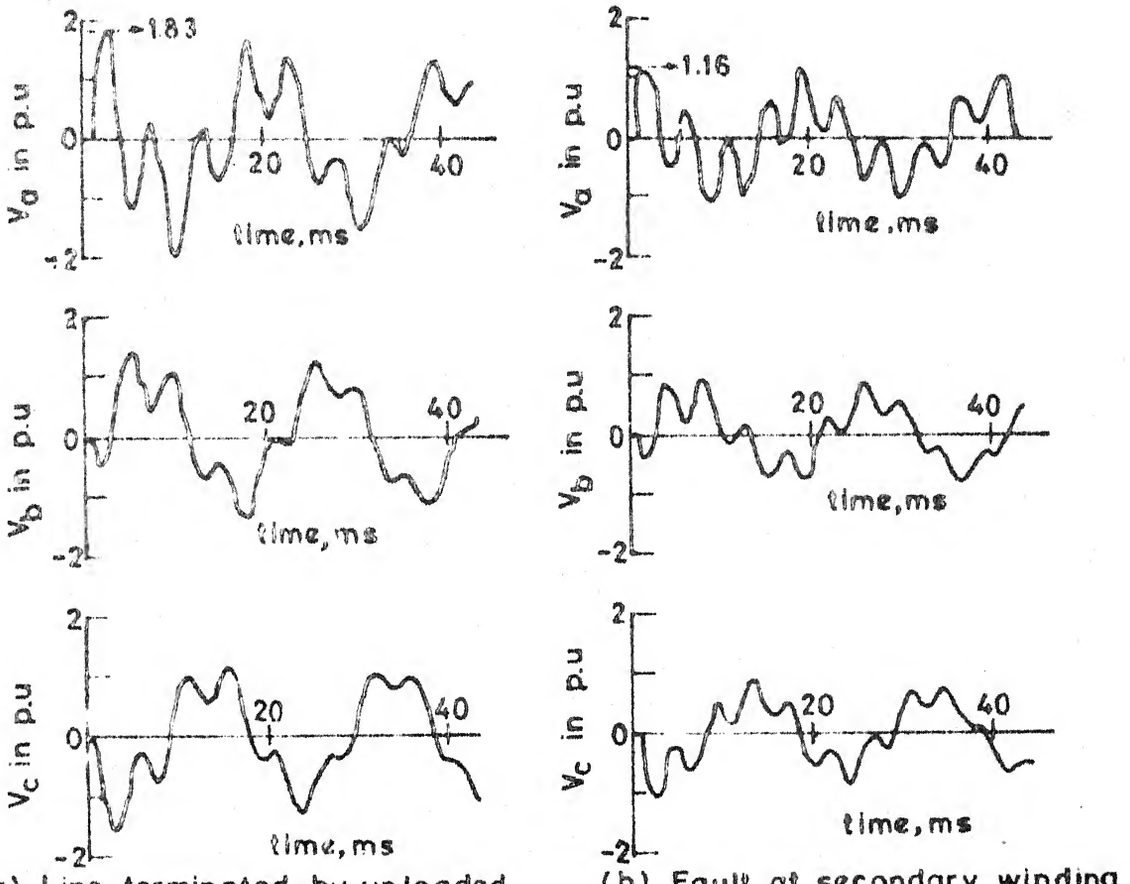

(a) Line terminated by unloaded transformer

(b) Fault at secondary winding of transformer

FIG 3.16 RECEIVING END VOLTAGES OF 400 kV, 230 km TRANSFORMER TERMINATED LINE. ANGLE OF SWITCHING: 90°, -30°, 210° OF PHASES a, b AND c RESPECTIVELY

In Figure 2.3, has been used. High voltage shunt reactors were connected at the sending and receiving ends of the line. The shunt reactor is represented by an equivalent inductance L_s whose values depend on degree of compensation i.e., reactive power of the reactor. The system at the sending end, with shunt reactor L_s connected to line, is now represented in Figure 3.17 by a Thevenin's equivalent having a voltage source E'_g and an impedance given by the following expressions:

$$E'_g = \frac{jWL_s}{R_g + jW(L_s + L_g)} E_g$$

$$= \frac{WL_s E_g \angle\theta}{\sqrt{R_g^2 + W^2(L_s + L_g)^2}} \qquad (3.15$$

Here $\theta = 90° - \tan^{-1}\left[\frac{W(L_g + L_s)}{R_g}\right]$

and $R'_g + jWL'_g = \frac{WL_s \sqrt{R_g^2 + W^2L_g^2}\ \angle(\theta_1 + 90°)}{\sqrt{R_g^2 + W^2(L_g + L_s)^2}\ \angle\theta_2}$

where $\theta_1 = \tan^{-1}\left[\frac{WL_g}{R_g}\right]$

$$\theta_2 = \tan^{-1}\left[\frac{W(L_g + L_s)}{R_g}\right]$$

$$\therefore\ R'_g = \frac{WL_s \sqrt{R_g^2 + W^2L_g^2}}{\sqrt{R_g^2 + W^2(L_g + L_s)^2}} \sin(\theta_2 - \theta_1) \qquad (3.16$$

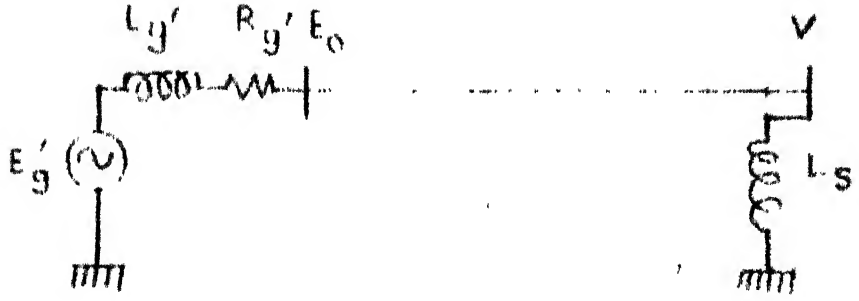

Fig. 3.17 Thevinins equivalent of the shunt compensated line.

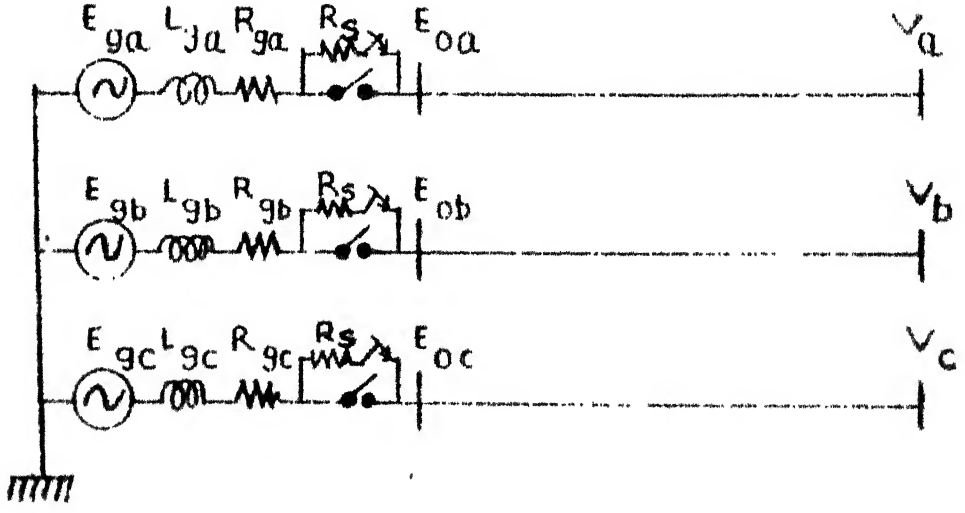

Fig. 3.18 Equivalent circuit of an unloaded line with pre-insertion resistor.

$$\text{and} \qquad L'_g = \frac{L_s \sqrt{R_g^2 + W^2 L_g^2}}{\sqrt{R_g^2 + W^2 (L_g + L_s)^2}} \cos(\theta_2 - \theta_1) \qquad (3.17)$$

Here

$$[E'_g] = \begin{bmatrix} E_{ga} \angle\theta \\ E_{gb} \angle\theta \\ E_{gb} \angle\theta \end{bmatrix}$$

$$[R'_g] = \begin{bmatrix} R'_{ga} & 0 & 0 \\ 0 & R'_{gb} & 0 \\ 0 & 0 & R'_{gc} \end{bmatrix} \quad \text{and} \quad [L'_g] = \begin{bmatrix} L'_{ga} & 0 & 0 \\ 0 & L'_{gb} & 0 \\ 0 & 0 & L'_{gc} \end{bmatrix}$$

The elements of matrices $[E'_g]$, $[R'_g]$ and $[L'_g]$ are given by equations (3.15), (3.16) and (3.17) respectively.

The receiving and sending end voltages for a shunt compensated line can be calculated by similar equations as outlined in Section 3.6 for an inductive-load terminated line. However, $[E_g]$, $[R_g]$ and $[L_g]$ will now have to be replaced by matrices $[E'_g]$, $[R'_g]$ and $[L'_g]$ respectively which are as defined above. The reactor at the receiving end has been treated as an equivalent load.

The receiving end voltages for the 220 kV, 250 km line with 100% compensation have been calculated and the waveforms obtained are shown in Figure 3.19(a). The maximum overvoltage in this case is found to be 1.84 p.u.

The receiving end voltage waveforms of 400 kV, 230 km line with shunt reactor compensation at both ends of

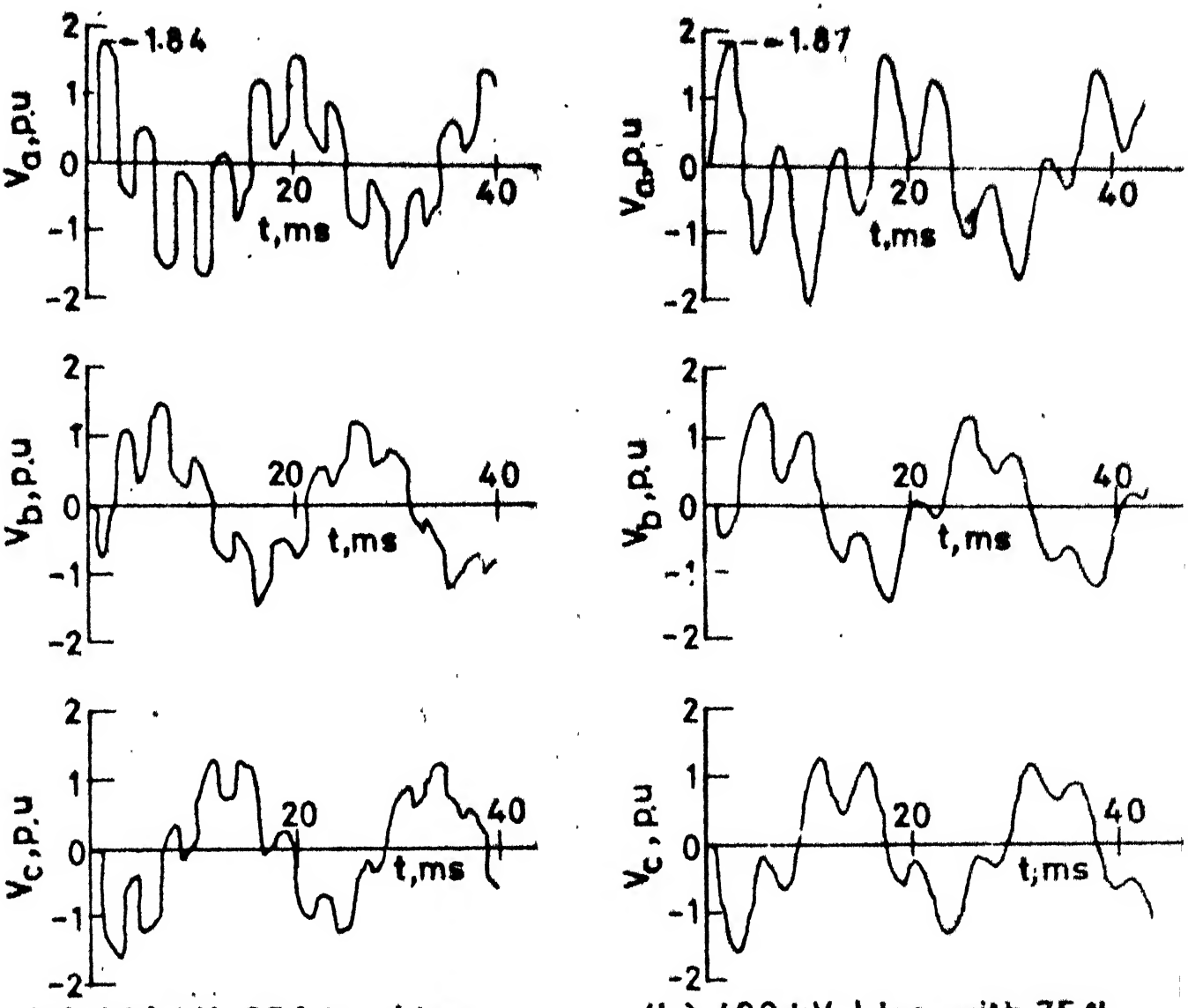

(a) 220 kV, 250 km Line
100 % Compensation
L_s = 9.26H

(b) 400 kV Line with 75 %
Compensation

FIG. 3.19 RECEIVING END VOLTAGES OF UNLOADED LINE WITH SHUNT REACTOR COMPENSATION

the line are shown in Figure 3.19(b). The amount of compensation used in the above case was 7.5% and the corresponding shunt reactor inductance (L_s) was 10.2 H. The maximum overvoltage for this condition is found to be 1.87 p.u. as opposed to 1.92 p.u. for the uncompensated line. Thus with shunt compensation, the overvoltage magnitude is found to decrease.

3.9 Effect of Pre-insertion Resistor:

The magnitude of switching overvoltage is an important factor in determining the air gap clearances of transmission line and the insulation level required. Hence it is desirable to reduce the magnitude of the switching overvoltage. The most effective means for achieving substantial reductions in switching overvoltages appearing on transmission line is by providing pre-insertion resistors across the main circuit breaker contacts [7, 12, 23]. In this section, the switching overvoltages occurring only on unloaded lines have been considered because this particular case has been found to give relatively high voltage stress on the system. The equivalent circuit of the system studied is shown in Figure 3.18. In this figure R_s represents the pre-insertion resistor.

The elements of matrix $[R_g]$, at the instant of switching will include both source resistance as well as pre-insertion resistance while at the end of insertion time the elements of $[R_g]$ include the source resistances alone.

The receiving end voltages of the 400 kV line have been calculated for several combinations of pre-insertion resistors and for various switching instants. It has been found that a 360 ohm resistor inserted in each phase at the instant of closing of the circuit breakers, reduces the overvoltage to 1.51 p.u. The receiving end voltage waveforms of the above line with pre-insertion resistor of 360 ohm inserted for 10 ms are shown in Figure 3.20(a). The maximum overvoltage is found to be 1.51 p.u. However, when a resistor of 320 ohm with an insertion time of 10 ms is used along with shunt compensation, the maximum overvoltage reduces further to 1.50 p.u.

The effect of closing resistors on the voltage magnitudes of 220 kV, 100 km unloaded line is shown in the Figure 3.20(b). It is seen that by inserting a resistor of 200 ohm for 10 ms, the overvoltage decreases to 1.50 p.u. Thus by using pre-insertion resistors a significant reduction in the overvoltage was found.

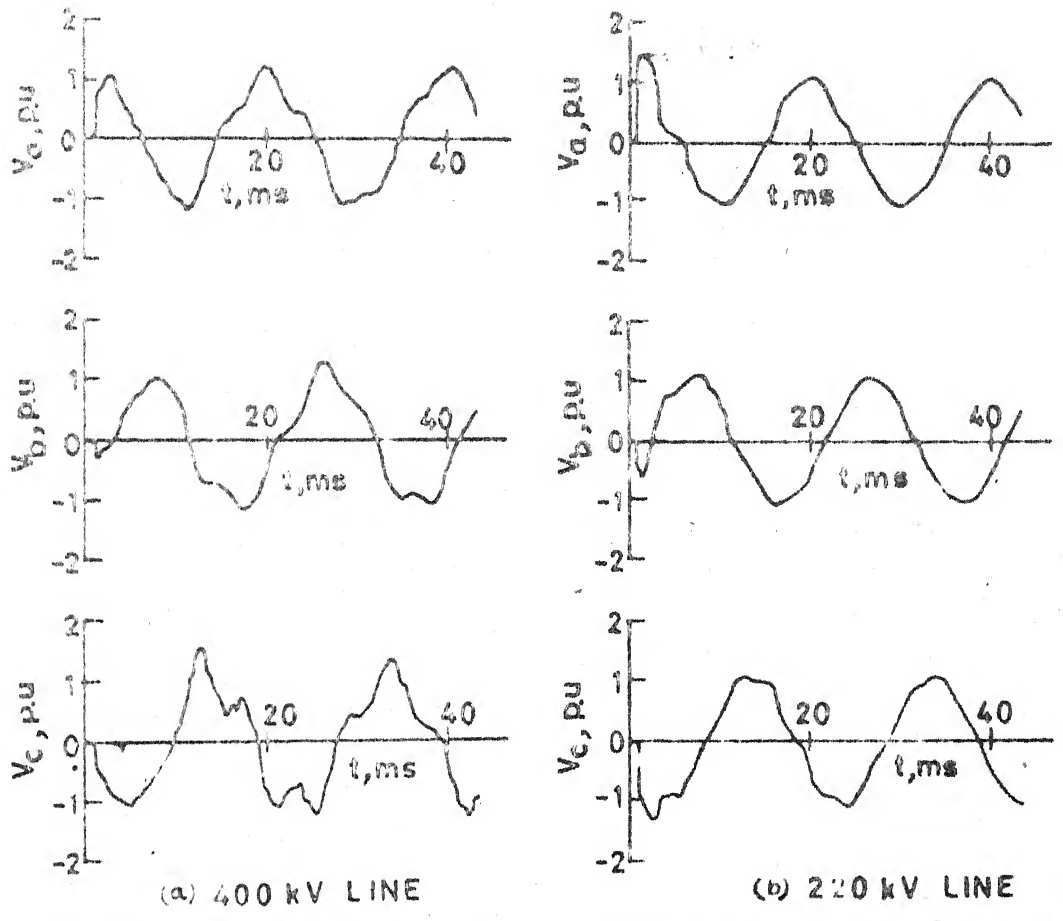

FIG 3.20 RESPONSE OF UNLOADED LINE WITH PRE-INSERTION RESISTOR

CHAPTER 4

PHASE TO PHASE SWITCHING OVERVOLTAGE

4.1 Introduction

Study of phase to phase switching overvoltage is necessary in order to find the minimum clearance between the conductors. Also, the magnitude of phase to phase switching overvoltage is an important factor in determining the size of the tower window, the number of insulators required and the cost of the transmission line supporting structures. The phase to phase clearance is necessarily greater than twice the phase to ground clearance [6].

A number of investigations on the TNA, as well as in real networks, have shown that the phase to ground overvoltages of two phases in the same system nearly always have opposite polarity at the time at which the overvoltages reach their peak values [7]. This means, that the overvoltage stress between two phases is generally much higher than that to ground but lower than twice the maximum phase to ground overvoltage stresses.

In this chapter, phase to phase switching overvoltages have been studied by using digital computer program as well as on the Transient Network Analyser. The different system conditions that have been taken into account are, unloaded line, resistive-load terminations, inductive-load termination and transformer terminations. The effect of source impedance and transformer winding connections on overvoltage

magnitude have also been studied. Switching surge control using shunt compensation and preinsertion resistors and their effects on the voltage magnitude have also been investigated. The phase to phase overvoltages are expressed as the ratio of the maximum peak value of phase to phase overvoltage to the peak value of reference power frequency voltage.

4.2 TNA Studies of Phase to Phase Overvoltage:

TNA experiments have been performed on the 220 kV line whose details are given in Appendix-E. The phase to phase voltage is obtained as the vector difference of two phase to ground voltages.

4.2.1 Overvoltage on Unloaded Line:

The equivalent circuit of the system studied is shown in Figure 3.3. The receiving end phase to phase voltage waveforms for a line of 250 km length, taking the source impedance into account are shown in Figure 4.1. The data of source impedance has been given in Appendix-E. The maximum phase to phase overvoltage, when all the three phases are switched simultaneously with phase 'a' at 60° position, is found to be 3.28 p.u. For the above switching position, the ratio of the phase to phase overvoltage to phase to neutral overvoltage is observed to be 1.65 p.u.

The effect of short-circuit power of the source behind the line, on phase-to-phase overvoltage for the 250 km line was observed and results are given below:

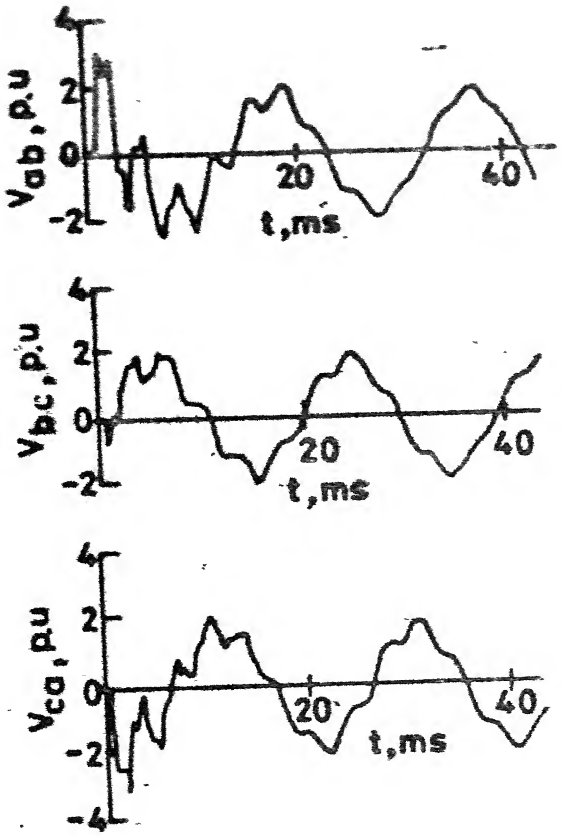

FIG. 4.1 RECEIVING END PHASE TO PHASE VOLTAGES OF 220 kV UNLOADED LINE . ANGLE OF SWITCHING: 60°,-60° & 180°

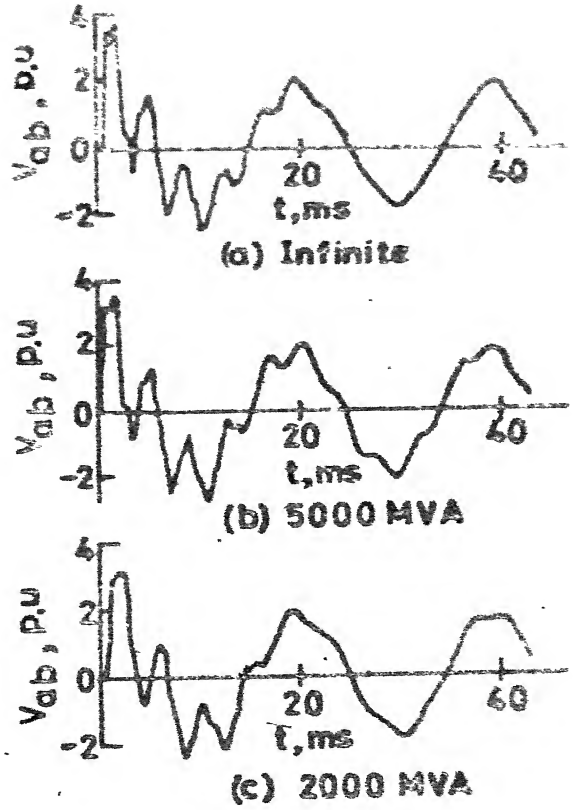

FIG. 4.2 PHASE TO PHASE VOLTAGES FOR VARIOUS SHORT CIRCUIT POWER

Short circuit MVA	Infinite	5000	2000	1000
Phase to phase over-voltage in p.u.	3.68	3.38	3.25	3.13

For the different values of short circuit MVA, the voltage waveforms are shown in Figure 4.2. It is seen that with the increase in source short-circuit power, the phase to phase overvoltages increases.

4.2.2 Effect of Shunt Reactor:

The effect of shunt reactor on phase to phase over-voltage magnitude was observed on the TNA. The equivalent circuit of the system studied is shown in Figure 2.3. The following results were obtained for the 250 km line length.

Percentage of compensation	0	90	100
Phase to phase overvoltage in p.u.	3.50	3.27	3.23

It is seen that, with the increase in the percentage of compensation, phase to phase overvoltage decreases.

4.2.3 Transformer Terminated Lines:

In order to study the phase to phase switching overvoltage for a transformer terminated line, three single phase miniature transformers were connected to form a three-phase transformer bank. The effects of transformer winding connections and excitation levels on the phase to phase overvoltage were studied. The excitation levels considered on the linear portion of the magnetization characteristic are 0.65% and 1.45% while those considered on the non-linear

portion of the magnetization curve are 2.6% and 15%. The various levels of excitation current were obtained by varying the system operating voltage.

The results obtained for a 220 kV, 250 km line are shown in Table 7.

Table 7

Phase to phase switching overvoltages of transformer terminated line

Transformer connection	Percentage of excitation	Phase to phase overvoltage in p.u.
Star-Delta	0.65	2.07
	1.45	2.38
	2.60	2.46
	15.00	2.50
Delta-Star.	0.65	1.64
	1.45	1.81
	2.60	1.84
	15.00	1.88

From the results given in the above table, it can be seen that the phase to phase overvoltage, with the transformer primary connected in star and the secondary in delta was found to be higher as compared with the case when primary is connected in delta and secondary in star. It was also found that the rise in overvoltage decreases as the level of excitation is increased.

4.3 Digital Calculation of Phase to Phase Overvoltages:

For the 400 kV line, whose details are given in Appendix-E, the phase to phase overvoltages have been calculated using digital computer. These calculations have been done by using the algorithm described in Section 3.2. As the phase to phase voltages V_{ab}, V_{bc} and V_{ca} consists of individual phase to neutral components, they are obtained in computer program by finding the difference between the corresponding phase-to-neutral components V_a, V_b and V_c.

4.3.1 Unloaded Line:

The phase to phase switching overvoltage of the 400 kV unloaded line have been calculated. Figure 3.3 shows the equivalent circuit of the system studied. The calculation is based on the same technique as illustrated in Section 3.4 for the computation of the phase to neutral voltages of an unloaded line with source impedance considered. The receiving end phase to phase voltage waveforms are shown in Figure 4.3. The maximum overvoltage is found to be 3.52 p.u.

4.3.2 Simple Line Terminations:

In this section, the phase to phase switching overvoltages of the 400 kV line terminated with resistive and inductive loads are calculated by following the methods outlined in Sections 3.5 and 3.6 respectively. The receiving end voltage waveforms, when the line is terminated with a resistive load of 400 MW is shown in Figure 4.4(a), while

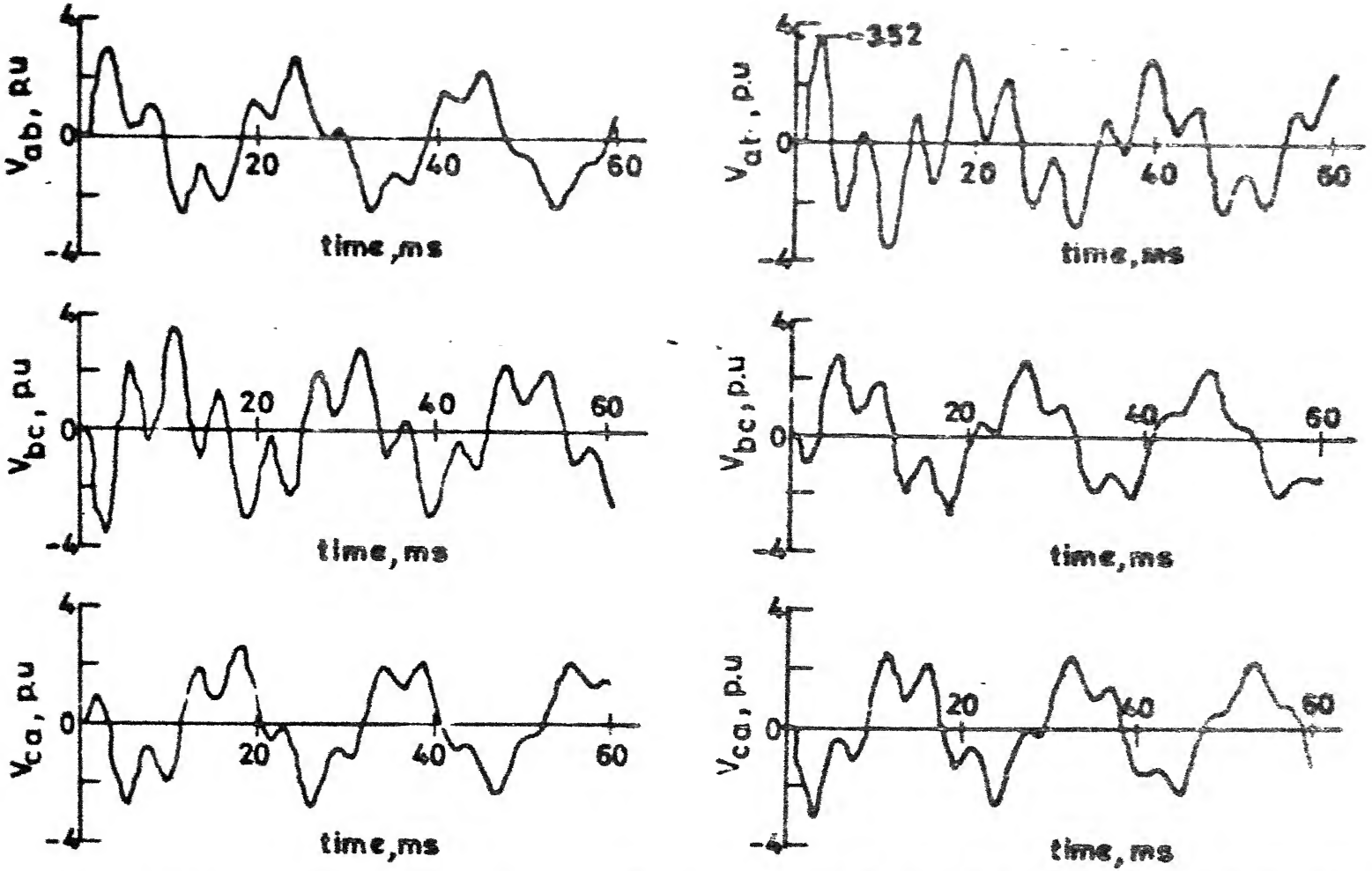

(a) Angle of switching : 0°, -120° & 120° (b) Angle of switching : 60°, -60° & 180°

FIG. 4.3 RECEIVING END PHASE TO PHASE VOLTAGE OF 400 kV UNLOADED LINE

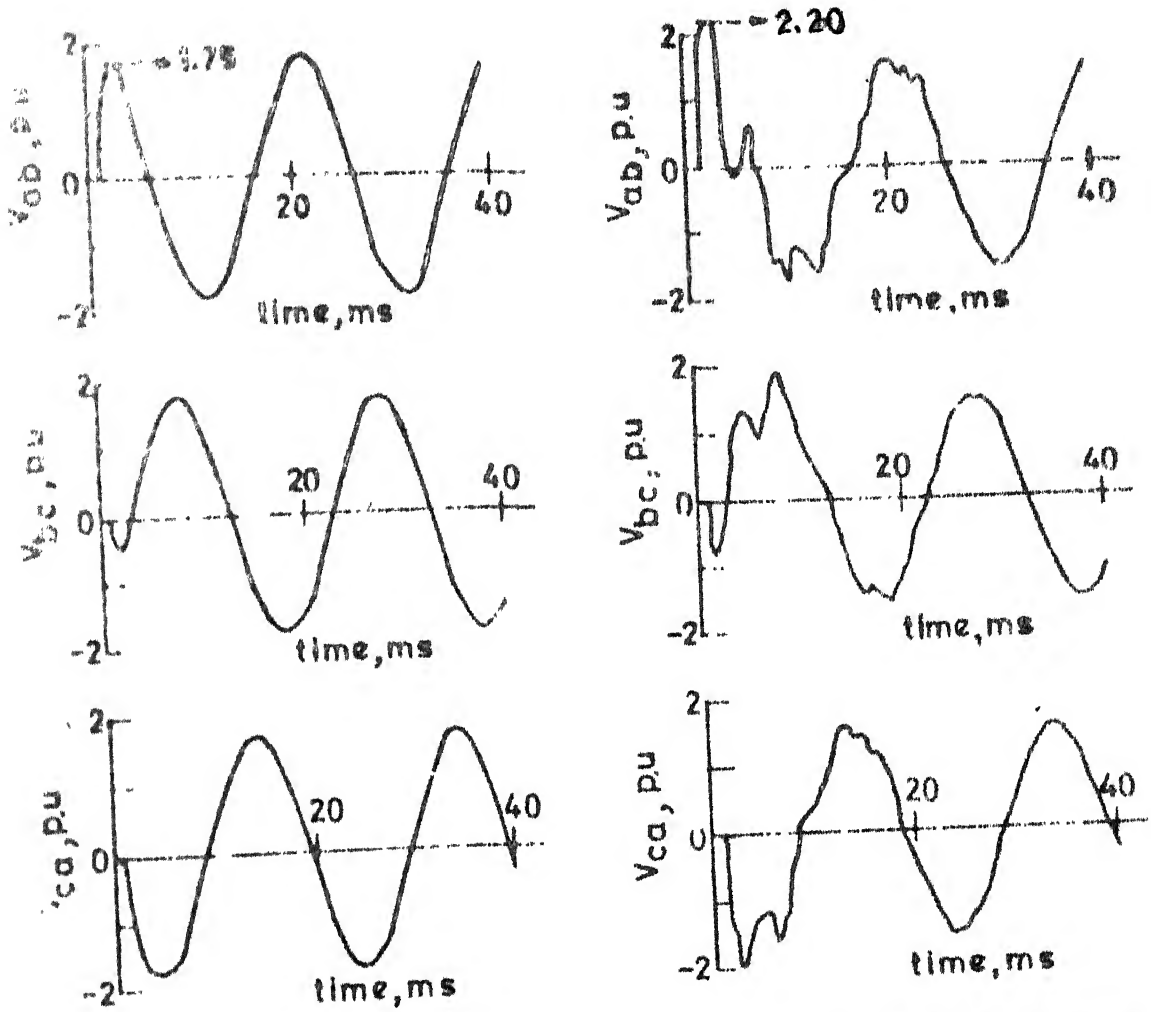

(a) Resistive load

(b) Inductive load

FIG 4.4 RECEIVING END PHASE TO PHASE VOLTAGES OF
400kV LINE . ANGLE OF SWITCHING : 60°,-60° & 18

the waveforms for an inductive load of the same value having a power factor of 0.9 is shown in Figure 4.4(b).

The maximum overvoltage for the resistive and the inductive load terminations are found to be 1.75 p.u. and 2.20 p.u. respectively. These are less than those for unloaded lines.

4.3.3 Transformer Terminated Line:

The phase to phase overvoltages of the 400 KV line, terminated at the receiving end with a 480 MVA unloaded transformer have been calculated. The resulting voltage waveforms are shown in Figure 4.5(a). In this case, the maximum overvoltage is found to be 3.31 p.u.

The phase to phase overvoltages for the condition of short circuited secondary are also calculated. The receiving end voltage waveforms for the same line terminated with a 100 MVA transformer whose secondary is short circuited, are shown in Figure 4.5(b). The maximum overvoltage is found to be 2.20 p.u.

4.3.4 Switching Surge Control:

With the advent of EHV system, it becomes technically and economically desirable to control and reduce switching surge severities. This is achieved by the inclusion of shunt reactors, and through the use of circuit breakers with pre-insertion resistors. The effect of shunt reactor compensation and pre-insertion resistors on the

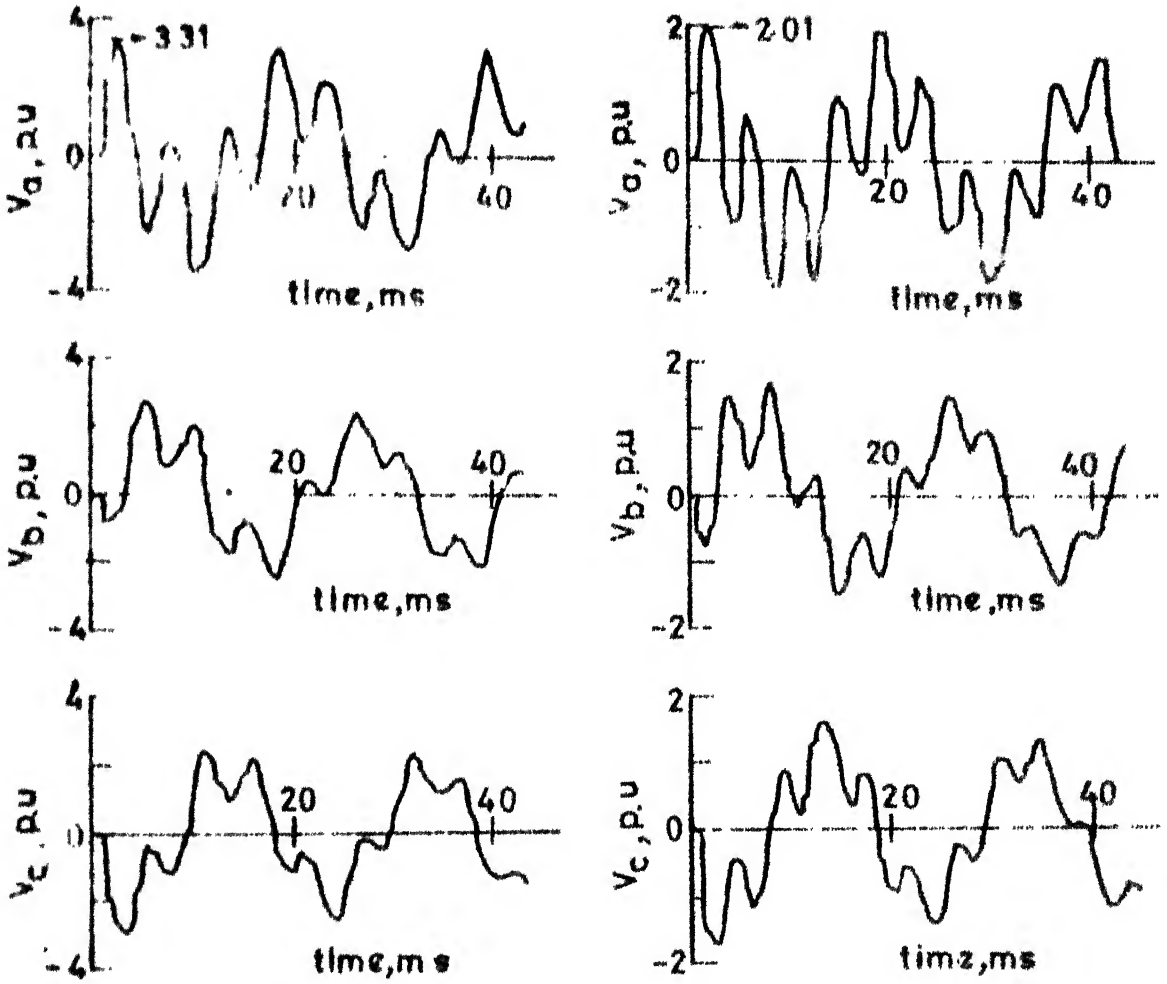

(a) Unloaded transformer (b) Fault at secondary

FIG 4.5 RECEIVING END PHASE TO PHASE VOLTAGES OE 400 k
TRANSFORMER TERMINATED LINE. ANGLE OF SWITCH
60°, -60° & 180°

overvoltage magnitude have been studied only for the 400 kV line.

(a) Shunt reactor compensation: The phase to phase switching overvoltage calculations with the shunt reactors included have been done by following a similar procedure as outlined in Section 3.8.

The receiving end voltage waveforms for 75% compensation are shown in Figure 4.6(b). The maximum overvoltage is found to be 3.25 p.u. Thus, the presence of shunt reactor reduces the overvoltage from 3.52 p.u. to 3.25 p.u.

(b) Pre-insertion resistor: The phase to phase voltages of the 400 kV unloaded line have been calculated by inserting a resistance of 360 ohm for a period of 10 ms. The results of calculation are shown in Figure 4.6(a). From this, the maximum overvoltage is found to be 2.54 p.u.

The phase to phase overvoltages of the above line with both shunt reactor compensation as well as with pre-insertion resistor have also been calculated. The maximum overvoltage, with 75% compensation and with 360 ohm pre-insertion resistor for an inserting period of 10 ms, is found to be 2.29 p.u.

From the above results it is clear that, overvoltage on transmission lines which can be as high as three to four times the normal operating voltage can be reduced considerably by providing pre-insertion resistors for a short duration.

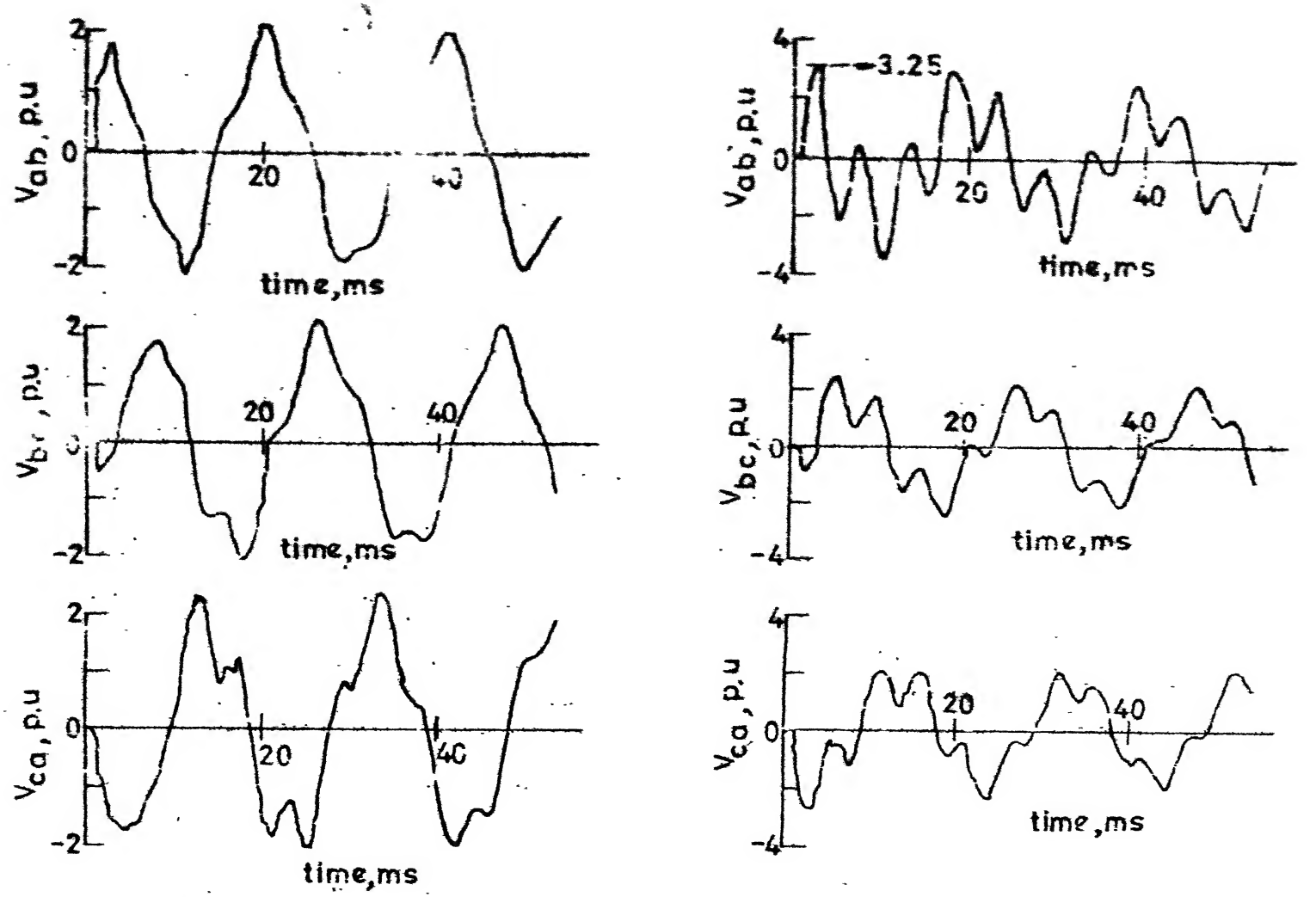

(a) With preinsertion resistor

(b) With shunt reactance compensation

FIG: 4.6 RECEIVING END PHASE TO PHASE VOLTAGES OF 400 kV UNLOADED LINE ANGLE OF SWITCHING : 60°,-60° & 180°

CHAPTER 5

CONCLUSION

This work is mainly devoted to the study of phase to neutral and phase to phase switching overvoltages arising due to energisation of 220 kV and 400 kV transmission lines. A computer program for calculating the switching overvoltages for different system conditions has been developed. The results of digital calculation for the 220 kV line were compared with the experimental results obtained from the Transient Network Analyser and the two were found to be in close agreement. The results obtained from this study will provide useful guidelines in determining the required insulation level.

From the TNA studies conducted on the 220 kV line, it was observed that the presence of source impedance decreases the overvoltage magnitude and also smoothens the voltage wave shape. It was also observed that the switching surge magnitude increases with the increase of short-circuit power and line length. For the same amount of load, the overvoltage magnitude on the line with resistive load was found to be lower than that for a line with inductive load. In the case of transformer terminated lines, for the two line lengths considered for various excitation levels of the transformer, the overvoltage in all the phases, with the primary of the transformer connected in delta and the secondary in star was found to be lower as compared with the case

when the primary is connected in star and secondary in delta. Further, with the increase in the size of transformer, the phase to neutral overvoltage was observed to decrease. Shunt reactors have been found to be quite effective in lowering the switching overvoltage magnitudes.

From the digital calculations performed for the 400 kV lines, it was found that the maximum switching overvoltage occurred on closing the lines at no-load. Further, it was also observed that energisation of an unloaded line with non-simultaneous closure of circuit breakers produced larger magnitude of overvoltage than for simultaneous closure of the breakers. However, for the resistive and inductive load terminated lines, there was no significant difference in the overvoltage magnitudes for the case of simultaneous and non-simultaneous closure of breakers. A substantial reduction in the overvoltage magnitude was obtained by introducing pre-insertion resistors rather than using shunt compensation. When pre-insertion resistors are considered, a greater reduction of switching surge was obtained for a compensated line as compared to an uncompensated line. For the same overvoltage magnitude, the resistor value was found to be lower for the compensated lines.

The phase to phase switching overvoltage was found to be higher on energizing an unloaded line as compared with that for resistive and inductive load terminated lines.

REFERENCES

1. R.D. Begamudre, "Design consideration for coils for transient network analyser for representing long lines". CPRI, Technical Report No. 107, pp. 3-5, May, 1981.

2. Alam Greenwood, "Electrical transients in power system". John Wiley and Sons, 1971, pp. 193-215.

3. R. Uram and R.W. Miller, "Mathematical analysis and solutions of transmission line transients-I theory", IEEE Trans. on Power Apparatus and System, Vol. PAS-83, pp. 1116-1123, Nov. 1964.

4. R. Uram and W.E. Ferro, "Mathematical analysis and solutions of transmission line transients-II applications", IEEE Trans. on Power Apparatus and Systems, Vol. PAS-83, pp. 1123-1136, Nov. 1964.

5. L.V. Beweley, "Travelling waves on transmission system", Dover Publications, Inc., 1951, pp. 291-349.

6. C. Menemenlis, H. Anis, and G. Harbec, "Phase to phase insulation Part-II: Required clearances and co-ordination with phase to ground insulation", IEEE Trans. on Power Apparatus System, Vol. PAS-95, No. 2, pp. 651-657, March/April 1976.

7. Ahdab M.K. El-Morshedy, "Phase to phase switching surges on 500 kV unloaded transmission line", IEE Proc., Vol. 129, pp. 199-205, Sept. 1982.

8. I.B. Johonson, R.F. Silva and D.D. Wilson, "Phase to phase switching surges on line energization", AIEE Transactions, Part-III (Power Apparatus and System), Vol. 81, pp. 298-302, Aug. 1962.

9. D.D. Wilson, "Phase to phase and phase-neutral switching surges on 500 kV open ended lines", IEEE Trans. Power Apparatus and System, Vol. PAS-88, No. 5, pp. 660-665, May 1969.

10. D.D. Wilson, "Phase to phase switching surges on 500 kV transformer terminated lines, Part-I: 500 kV circuit breaker operations", IEEE Trans. Power Apparatus and System, Vol. PAS-89, No. 5/6, May/June 1970.

11. J. Sabath, "Analog computer study of switching surge transients for a 500 kV system", IEEE Trans. on Power Apparatus and System, Vol. PAS-85, No. 1, pp. 1-9, Jan. 1966.

12. Paul A. Battensperger and Peter Djurdjevic, "Damping of switching overvoltages in EHV networks, New Economic Aspects and Solutions", IEEE Trans. on Power Apparatus and System, Vol. PAS-88, No. 7, pp. 1014-1021, July 1969.

13. R.G. Colclaser, C.L. Wagnar and E.P. Donohne, "Multi-step resistor control of switching surges", IEEE Trans. on Power Apparatus and System, Vol. PAS-88, No. 7, pp. 1022-1028, July 1969.

14. Sujatha Subhash, K.S. Meera and M. Kanya Kumari, "Switching overvoltage study on transmission lines with complex termination by TNA models and digital calculation", Proceedings of the Fiftieth Research and Development Session, pp. 73-81, March 1983.

15. A.C. Legate, "Comparison of field switching surge measurements with TNA measurements", IEEE Trans. on Power Apparatus and System, Vol. PAS-90, pp. 1347-1354, May/June, 1971.

16. A. Clerici, G. Ruckstuhl and A. Vian, "Influence of shunt reactors on switching surges", IEEE Trans. on Power Apparatus and System, Vol. PAS-70, pp. 1727-1736, Nov./Dec. 1970.

17. IEEE Committee Report, "Switching surges, Part-III: Field and analyser results for transmission line: Past, Present and Future Trends", IEEE Trans. Power Apparatus and System, Vol. PAS-89, pp. 173-189, Jan. 1970.

18. A. Colombo, G. Sartoria and A. Taschini, "Phase to phase air clearances in EHV substations as required by switching surge", CIGRE, Paper 33-11, 1972.

19. L. Paris, "Basic consideration of magnitude reduction of switching surges due to line energization", IEEE Trans. Power Apparatus and System, Vol. PAS-87, pp. 295-305, Jan. 1968.

20. H.B. Thoren, "Reduction of switching overvoltages in EHV and UHV system", IEEE Trans. Power Apparatus and System, Vol. PAS-90, Part-I, pp. 1321-1333, May/June 1971.

21. E. Clarke, H.A. Peterson and P.H. Light, "Abnormal voltage conditions in three phase systems produced by single-phase switching", AIEE Transaction, Part-III (Power Apparatus and System), Vol. 60, pp. 329-339, 1941.

22. L.P. Singh, "Advanced power system analysis and dynamics", Wiley Eastern Limited, 1983, pp. 168-177.

23. O.I. Elgerd, "Electric energy systems theory: An introduction", Tata McGraw-Hill Publishing Company Ltd., TMH edition, 1983, pp. 186-213.

24. E.E. Hedman, C.H. Titus and D.D. Wilson, "Switching of extra high voltage circuits, Part-II, Surge reduction with circuit breaker resistors", IEEE Trans. Power Apparatus and System, Vol. PAS-83, pp. 1196-1204, Dec. 1964.

APPENDIX A

DIMENSIONS OF DIFFERENT LINE CONFIGURATION

Dimensions and other details of the U.P. 400 kV line and the 735 kV lines are given below.

(i) U.P. 400 kV Single-Circuit Line:

Radius of the sub-conductor = 0.0159 m

Bundle spacing = 0.4572 m

Number of sub-conductors = 2

Phase spacing = 11 m

Minimum line to ground clearance = 9 m

Sag = 12 m

Average line height = 13 m

Line configuration : Horizontal

(ii) 735 kV Single-Circuit Line:

Radius of the sub-conductor = 0.0176 m

Bundle spacing = 0.4572 m

Number of sub-conductors = 4

Phase spacing = 15.24 m

Average line height = 13.8 m

Line configuration : Horizontal

APPENDIX B

DETERMINATION OF LINE PARAMETERS

Bundle conductors are used in EHV lines to reduce the conductor surface gradient. The bundle is represented by an equivalent conductor of radius R_{eq} given by

$$R_{eq} = R' \times (n \times r/R')^{1/n} \qquad (B.1)$$

where,

r - radius of sub-conductor

R' - radius of bundle

n - number of sub-conductors in the bundle.

The diagonal elements of the inductance matrix are given by

$$L'_{ii} = 0.2 \, \mathrm{Log}_e(2H/R_{eq}) \qquad (B.2)$$

and the off-diagonal elements are

$$L'_{ij} = 0.2 \, \mathrm{Log}_e(D'_{ij}/D_{ij}) \qquad (B.3)$$

$$i \neq j$$

where,

L' - inductance in mH/km

H - average height of the conductor above the ground in metres

R_{eq} - equivalent radius of the conductor in metres

D'_{ij} - aerial distance between conductor i and the image of the jth conductor

D_{ij} - distance between the conductors i and j.

The capacitance matrix C is obtained from the inductance matrix, by assuming the velocity of wave is equal to the light velocity; i.e.,

$$v^2 = \frac{1}{LC} \tag{B.4}$$

where, v is the velocity of light

or
$$[C] = \frac{1}{v^2}\left[L'\right]^{-1} \tag{B.5}$$

The positive sequence inductance L_1 and the positive sequence capacitance C_1 are given by

$$L_1 = L'_s - L'_m$$
$$\text{and} \quad C_1 = C_s - C_m \tag{B.6}$$

where,

C_s - self capacitance between the line and ground

C_m - mutual capacitance between the lines

L'_s - self inductance

L'_m - mutual inductance.

APPENDIX C

DESIGN OF COILS FOR REPRESENTING TRANSMISSION LINE MODEL

Design of the coil for representing the transmission line has been done on the basis of Brook's coil representation [1] which is shown in Figure C.1.

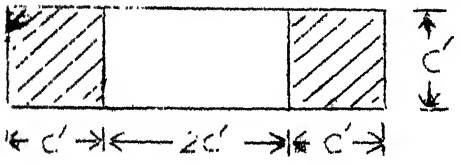

Figure C.1. Brook's coil

The coil has a square cross-section of side C' with a winding of inner diameter 2C', outer diameter 4C' and mean diameter 3C'. Dimensions of the coils are dependent on the ratio of its inductance to resistance. The inductance of the coil whose major dimension C' is in cm; is given by

$$L = 0.0255\ C'N_1^2 \text{ microhenry} \qquad (C.1)$$

Here, N_1 is the number of turns in the coil and can be written as

$$N_1 = \left(\frac{C'}{d}\right)^2 \qquad (C.2)$$

where, d is the diameter of the wire in cm.

The resistance of the coil is

$$R = 1.7 \times 10^{-6} \times \pi \times 3C' \times N_1/\left(\frac{\pi d^2}{4}\right)$$

$$= 20.4 \times 10^{-6} \times N_1 C'/d^2 \text{ ohm} \qquad (C.3)$$

From equations (C.1) and (C.2)

$$L = 0.0255 \times \frac{C'^5}{d^4} \text{ microhenry}$$

$$= 2.55 \times 10^{-8} \times \frac{C'^5}{d^4} \text{ Henry} \qquad (C.4)$$

The time constant of the coil

$$= L/R = \frac{C'^2}{800} \text{ seconds}$$

i.e. $$C' = [800 \times L/R]^{1/2} \text{ cm} \qquad (C.5)$$

where C', the major dimension of the coil is fixed for a coil representing certain section at a given transmission voltage level, however the number of turns will differ depending on the total inductance in the coil,

$$\text{Length of wire, } l = 3\pi C' N_1/100 \text{ meter} \qquad (C.6)$$

$$\text{Weight of coil} = = (\tfrac{\pi}{4})\, d^2 l \times 10^{-4} \times 8930 \text{ Kg}$$

$$= 1495.7 \times (\tfrac{L}{R})^{3/2} \text{ kg} \qquad (C.7)$$

Weight of the coil remains same as long as the ratio of its inductance to that of resistance remains constant, irrespective of the line length that it represents.

APPENDIX D

STEP RESPONSE OF AN OPEN ENDED LINE BY TRAVELLING-WAVE METHOD

Figure D.1 shows a single phase distributed parameter line whose receiving end is kept open

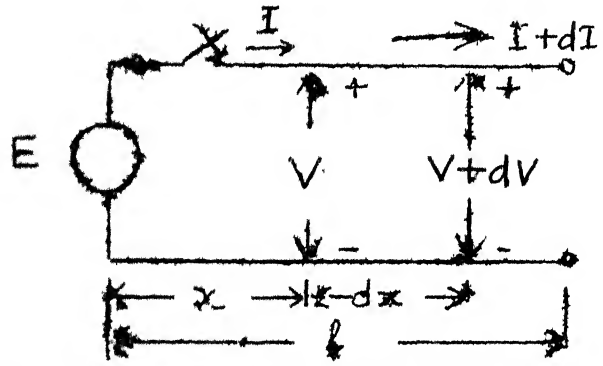

Figure D.1 Transmission line with distributed parameter.

The differential equation for current and voltages are

$$\frac{dv}{dx} = -zI \qquad (D.1)$$

$$\frac{dI}{dx} = -yV \qquad (D.2)$$

Here, $z = R + LS$ and $y = Cs$

where R, L and C are resistance, inductance and capacitance of the line per unit length respectively. s is the Laplace-Transform operator and l is the line length.

From equations (D.1) and (D.2) we get,

$$\frac{d^2V}{dx^2} = zyV = p^2V \qquad (D.3)$$

where, $p = \sqrt{zy}$ is the propagation factor.

The voltage and current at any point along the length of the line is given by,

$$V = A_1 e^{+px} + B_1 e^{-px} \qquad (D.4)$$

$$I = \frac{p}{R + sL} [- A_1 e^{px} + B_1 e^{-px}] \qquad (D.5)$$

At the sending end, $x = 0$ and $V = E$ while at the receiving end, $x = l$ and $I = 0$.

By introducing these initial conditions in equations (D.5) and (D.6) we get,

$$A_1 = \frac{Ee^{-pl}}{e^{pl} + e^{-pl}} \quad \text{and} \quad B_1 = \frac{Ee^{pl}}{e^{pl} + e^{-pl}}$$

Now, the voltage and current at any point of the line is given by,

$$V = \frac{2E \cosh p(l - x)}{e^{pl} + e^{-pl}} \qquad (D.6)$$

The voltage at the far end of the line i.e. at $x = l$ is

$$V(s, l) = \frac{2E(s)}{e^{pl} + e^{-pl}} \qquad (D.7)$$

Now, $p^2 = (R + sL)Cs$

$$= LC(s^2 + \frac{R}{L} s)$$

$$= \frac{1}{v^2} [(s + \frac{R}{2L})^2 - (\frac{R}{2L})^2] \qquad (D.8)$$

By neglecting the term $(R/2L)^2$ in equation (D.10) we get,

$$p = \frac{1}{v} (s + \frac{R}{2L}) = \frac{s}{v} + \frac{R}{2Z}$$

where $v = \frac{1}{\sqrt{LC}}$ is the velocity of propagation

and $Z = \sqrt{L/C}$ is the characteristic impedance of the line.

Now, $e^{pl} = e^{(\frac{sl}{v} + \frac{Rl}{2Z})} = A_o^{-1} e^{\frac{ls}{v}}$

where $A_o = e^{-\frac{Rl}{2Z}}$

The voltage at the open end of the line is

$$V(l,s) = \frac{2E(s)}{e^{pl} + e^{-pl}}$$

$$= 2E(s) [e^{-pl} - e^{-3pl} + e^{-5pl} - e^{-7pl} + \ldots]$$

In time domain, the open end voltage can be written as

$$V(l,t) = 2[A_o E(t - T_2) - A_o^3 E(t - 3T_2) + A_o^5 E(t - 5T_2) \ldots] \quad (D.9)$$

where $T_2 = l/v$, is the wave travel time.

The line parameters of the transmission line model developed in the laboratory are:

R_{dc} = 0.864 ohm/km

C_s = 7.88 nF/km

C_m = - 1.63 nF/km

C_1 = 9.51 nF/km and L_1 = 1.20 mH/km

line length, l = 60 km

Now, Travel time = $1/v$ = 0.202 ms

Surge impedance $= \sqrt{L_1/C_1} = 355$ ohm

and $A_o = 0.928$

For an unit step input, the open end voltages at different times are:

At $t = 0$, $V = 0$

$t = T_2$, $V = 1.85$

$t = 2T_2$, $V = 1.85$

$t = 3T_2$, $V = 0.26$

Using the above calculations, the step response of a distributed parameter line has been drawn in Figure 2.1(f).

APPENDIX E

SYSTEM DATA FOR OVERVOLTAGE STUDY

1) 220 kV System:

Transmission-line data	Zero-sequence	Positive-sequence
Resistance, ohm/km	0.34	0.0706
Inductance, mH/km	4.0	1.2533
Capacitance, nF/km	6.0	8.850
Surge impedance, ohm	815	376

Line length = 250 km and 100 km

Generator MVA = 1000

Source impedance = (0.0 + j 14.72) ohm

2) 400 kV System (Obra-Sultanpur Line):

Transmission-line data	Zero-sequence	Positive-sequence
Resistance, ohm/km	0.29	0.0325
Inductance, mH/km	3.077	1.053
Capacitance, nF/km	7.0	11.5
Surge impedance, ohm	663	302

Line length = 230 km

Generator MVA = 1000

Source impedance = (0.0 + j 52.0) ohm.

APPENDIX F

GENERAL SOLUTION OF THREE PHASE TRANSMISSION LINE EQUATIONS

The equivalent circuit of a 3-phase transmission line is shown in Figure 3.1. Two sets of equations are derived from the equivalent circuit. The first is found by applying Kirchoff's voltage law to the loop formed by each conductor and ground, while the second is written using Kirchoff's current law at the junction of each conductor with capacitive branch to ground. These equations after suitable manipulations may be written as:

$$-\frac{\partial E_a(x,t)}{\partial x} = \frac{1}{3}\{[(R_o + L_o\frac{\partial}{\partial t}) + 2(R_1 + L_1\frac{\partial}{\partial t})]\, I_a(x,t) + [(R_o + L_o\frac{\partial}{\partial t}) - (R_1 + L_1\frac{\partial}{\partial t})]\, I_b(x,t) + [(R_o + L_o\frac{\partial}{\partial t}) - (R_1 + L_1\frac{\partial}{\partial t})]\, I_c(x,t)\} \quad (F.1)$$

$$-\frac{\partial E_b(x,t)}{\partial x} = \frac{1}{3}\{[(R_o + L_o\frac{\partial}{\partial t}) - (R_1 + L_1\frac{\partial}{\partial t})]\, I_a(x,t) + [(R_o + L_o\frac{\partial}{\partial t}) + 2(R_1 + L_1\frac{\partial}{\partial t})]\, I_b(x,t) + [(R_o + L_o\frac{\partial}{\partial t}) - (R_1 + L_1\frac{\partial}{\partial t})]\, I_c(x,t)\} \quad (F.2)$$

$$-\frac{\partial E_c(x,t)}{\partial x} = \frac{1}{3}\{[(R_o + L_o\frac{\partial}{\partial t}) - (R_1 + L_1\frac{\partial}{\partial t})]\, I_a(x,t)$$

$$+\left[\left(R_o + L_o \frac{\partial}{\partial t}\right) - \left(R_1 + L_1 \frac{\partial}{\partial t}\right)\right] I_b(x,t)$$

$$+\left[\left(R_o + L_o \frac{\partial}{\partial t}\right) + 2\left(R_1 + L_1 \frac{\partial}{\partial t}\right)\right] I_c(x,t) \} \quad \text{(F.3)}$$

$$-\frac{\partial E_a(x,t)}{\partial t} = \frac{1}{3}\left[\left(\frac{1}{C_o} + \frac{2}{C_o}\right) \frac{\partial I_a(x,t)}{\partial x} + \left(\frac{1}{C_o} - \frac{1}{C_1}\right) \frac{\partial I_b(x,t)}{\partial x}\right.$$

$$\left. + \left(\frac{1}{C_o} - \frac{1}{C_1}\right) \frac{\partial I_c(x,t)}{\partial x}\right] \quad \text{(F.4)}$$

$$-\frac{\partial E_b(x,t)}{\partial t} = \frac{1}{3}\left[\left(\frac{1}{C_o} - \frac{1}{C_1}\right) \frac{\partial I_a(x,t)}{\partial x} + \left(\frac{1}{C_o} + \frac{2}{C_1}\right) \frac{\partial I_b(x,t)}{\partial x}\right.$$

$$\left. + \left(\frac{1}{C_o} - \frac{1}{C_1}\right) \frac{\partial I_c(x,t)}{\partial x}\right] \quad \text{(F.5)}$$

$$-\frac{\partial E_c(x,t)}{\partial t} = \frac{1}{3}\left[\left(\frac{1}{C_o} - \frac{1}{C_1}\right) \frac{\partial I_a(x,t)}{\partial x} + \left(\frac{1}{C_o} - \frac{1}{C_1}\right) \frac{\partial I_b(x,t)}{\partial x}\right.$$

$$\left. + \left(\frac{1}{C_o} + \frac{2}{C_1}\right) \frac{\partial I_c(x,t)}{\partial x}\right] \quad \text{(F.6)}$$

The partial differentials appearing in equations (F.1) to (F.6) are converted to ordinary differentials by taking the Laplace transform with respect to time. The results can be expressed in a compact form as;

$$-\begin{bmatrix} \frac{dE_a(x,s)}{dx} \\ \frac{dE_b(x,s)}{dx} \\ \frac{dE_c(x,s)}{dx} \end{bmatrix} = \frac{1}{3}\begin{bmatrix} z_o+2z_1 & z_o-z_1 & z_o-z_1 \\ z_o-z_1 & z_o+2z_1 & z_o-z_1 \\ z_o-z_1 & z_o-z_1 & z_o+2z_1 \end{bmatrix} \begin{bmatrix} I_a(x,s) \\ I_b(x,s) \\ I_c(x,s) \end{bmatrix} \quad \text{(F.7)}$$

$$-\begin{bmatrix} E_a(x,s) \\ E_b(x,s) \\ E_c(x,s) \end{bmatrix} = \frac{1}{3}\begin{bmatrix} \frac{1}{y_o}+\frac{2}{y_1} & \frac{1}{y_o}-\frac{1}{y_1} & \frac{1}{y_o}-\frac{1}{y_1} \\ \frac{1}{y_o}-\frac{1}{y_1} & \frac{1}{y_o}+\frac{1}{y_1} & \frac{1}{y_o}-\frac{1}{y_1} \\ \frac{1}{y_o}-\frac{1}{y_1} & \frac{1}{y_o}-\frac{1}{y_1} & \frac{1}{y_o}+\frac{1}{y_1} \end{bmatrix} \begin{bmatrix} \frac{dI_a(x,s)}{dx} \\ \frac{dI_b(x,s)}{dx} \\ \frac{dI_c(x,s)}{dx} \end{bmatrix} \quad (F.8)$$

where, z_o, z_1, y_o and y_1 are defined as

$$\begin{aligned} z_o &= R_o + sL_o \\ z_1 &= R_1 + sL_1 \\ y_o &= sC_o \\ y_1 &= sC_1 \end{aligned} \quad (F.9)$$

Equations (F.7) and (F.8) can be written as follows:

$$-\frac{d}{dx}[E(x,s)] = \frac{1}{3}[Z_A][I] \quad (F.10)$$

and

$$-E(x,s) = \frac{1}{3}[Z_B]\frac{d}{dx}[I] \quad (F.11)$$

Solution of equation (F.10) and (F.11) gives,

$$\frac{d^2}{dx^2}[E(x,s)] = [Z_A][Z_B][E(x,s)] = 0 \quad (F.12)$$

where

$$[Z_A][Z_B]^{-1} = \frac{1}{3}\begin{bmatrix} z_oy_o + 2z_oy_o & z_oy_o - z_1y_1 & z_oy_o - z_1y_1 \\ z_oy_o - z_1y_1 & z_oy_o + 2z_1y_1 & z_oy_o - z_1y_1 \\ z_oy_o - z_1y_1 & z_oy_o - z_1y_1 & z_oy_o - 2z_1y_1 \end{bmatrix} \quad (F.13)$$

Defining $$[P] = [Z_A][Z_B]^{-1}$$

Equation (F.12) now becomes,

$$\frac{d^2}{dx^2}[E(x,s)] - [P][E(x,s)] = 0 \qquad (F.14)$$

Equation (F.14) may be expanded into its components and written as;

$$\frac{d^2E_a(x,s)}{dx^2} - P_{11}E_a(x,s) - P_{12}E_b(x,s) - P_{13}E_c(x,s) = 0$$

$$\frac{d^2E_b(x,s)}{dx^2} - P_{21}E_a(x,s) - P_{22}E_b(x,s) - P_{23}E_c(x,s) = 0$$

$$\frac{d^2E_c(x,s)}{dx^2} - P_{31}E_a(x,s) - P_{32}E_b(x,s) - P_{33}E_c(x,s) = 0 \qquad (F.15)$$

The difficulty in solving equation (F.15) due to mathematical coupling between the voltages can be avoided if the off-diagonal elements of the P-matrix can be made zero. Then each equation would contain only one voltage and thus would be solvable. This can be done by transforming the transmission line voltage E(x,s) to a new set of variables F(x,s). Equation (F.14) will then be of the form;

$$\frac{d^2}{dx^2}[F(x,s)] - [Q][F(x,s)] = \bar{0} \qquad (F.16)$$

E(x,s) and F(x,s) are related by a transformation matrix [T] as;

$$[E(x,s)] = [T][F(x,s)] \qquad (F.17)$$

or, $$[F(x,s)] = [T]^{-1}\,[E(x,s)]$$

Substitution of equation (F.17) in equation (F.14) gives,

$$\frac{d^2}{dx^2}[F(x,s)] - [T]^{-1}[P][T][F(x,s)] = 0 \qquad \text{(F.18)}$$

Comparing equation (F.18) and (F.16) we get,

$$[\Omega] = [T]^{-1}[P][T] \qquad \text{(F.19)}$$

Now, with a proper transformation matrix, $[\Omega]$ will be diagonal. The transformation matrix $[T]$ can be found as follows:

1. The eigen values or the characteristic roots of the matrix $[P]$ is found.
2. The eigen vector corresponding to each eigen value is then computed. The column vectors of $[T]$ are proportional to the eigen vectors of the matrix $[P]$.

The matrix $[T]$ and its inverse found by following the steps outlined above, is given as

$$[T] = \begin{bmatrix} 1 & 1 & 0 \\ 1 & 0 & 1 \\ 1 & -1 & -1 \end{bmatrix} \qquad \text{(F.20)}$$

$$[T]^{-1} = \frac{1}{3}\begin{bmatrix} 1 & 1 & 1 \\ 2 & -1 & -1 \\ -1 & 2 & -1 \end{bmatrix} \qquad \text{(F.21)}$$

Substituting equations (F.20) and (F.21) in equation (F.19),

$$[Q] = [T]^{-1}[P][T] = \begin{bmatrix} z_o y_o & 0 & 0 \\ 0 & z_1 y_1 & 0 \\ 0 & 0 & z_1 y_1 \end{bmatrix} \qquad (F.22)$$

Substitution of equation (F.22) in equation (F.16) gives

$$\frac{d^2 F_a(x,s)}{dx^2} - (z_o y_o)\, F_a(x,s) = 0$$

$$\frac{d^2 F_b(x,s)}{dx^2} - (z_1 y_1)\, F_b(x,s) = 0 \qquad (F.23)$$

$$\frac{d^2 F_c(x,s)}{dx^2} - (z_1 y_1)\, F_c(x,s) = 0$$

Solution of these differential equation can be written as,

$$F(x,s) = [K_1 e^{-mx}] + [K_2 e^{mx}] \qquad (F.24)$$

where

$$[K_1 e^{-mx}] = \begin{bmatrix} K_{a1}\, e^{-\sqrt{z_o y_o}\, x} \\ K_{b1}\, e^{-\sqrt{z_1 y_1}\, x} \\ K_{c1}\, e^{-\sqrt{z_1 y_1}\, x} \end{bmatrix}$$

and

$$[K_2 e^{mx}] = \begin{bmatrix} K_{a2}\, e^{\sqrt{z_o y_o}\, x} \\ K_{b2}\, e^{\sqrt{z_1 y_1}\, x} \\ K_{c2}\, e^{\sqrt{z_1 y_1}\, x} \end{bmatrix} \qquad (F.25)$$

Substitution of equations (F.24) and (F.25) in equation (F.17) gives the solution for line voltages.

$$E(x,s) = [T][K_1 e^{-mx}] + [T][K_2 e^{mx}] \tag{F.26}$$

From equation (F.10), we get

$$\begin{aligned} I(x,s) &= -3[Z_A]^{-1} \frac{d}{dx}[E(x,s)] \\ &= -3[Z_A]^{-1}[T] \frac{d}{dx}\{[K_1 e^{-mx}] + [K_2 e^{mx}]\} \\ &= -3[T][T]^{-1}[Z_A]^{-1}[T] \frac{d}{dx}\{[K_1 e^{-mx}] + [K_2 e^{mx}]\} \end{aligned} \tag{F.27}$$

where,

$$[T]^{-1}[Z_A]^{-1}[T] = \begin{bmatrix} \frac{1}{3Z_o} & 0 & 0 \\ 0 & \frac{1}{3Z_1} & 0 \\ 0 & 0 & \frac{1}{3Z_1} \end{bmatrix} \tag{F.28}$$

Using equations (F.25), (F.27) and (F.28), the general expression for current can be written as,

$$I(x,s) = [T][Z]^{-1}[K_1 e^{-mx}] - [T][Z]^{-1}[K_2 e^{mx}] \tag{F.29}$$

where $[Z]$ is a diagonal matrix of the form,

$$[Z] = \begin{bmatrix} \sqrt{z_o/y_o} & 0 & 0 \\ 0 & \sqrt{z_1/y_1} & 0 \\ 0 & 0 & \sqrt{z_1/y_1} \end{bmatrix} \tag{F.30}$$

The elements of the matrix $[Z]$ are the characteristic impedance of the line. The exact form of the

characteristic impedance is complex, but if the line is lossless, the following expressions are obtained,

$$Z_o = \sqrt{z_o/y_o} = \sqrt{L_o/C_o}$$
$$Z_1 = \sqrt{z_1/y_1} = \sqrt{L_1/C_1} \qquad (F.31)$$

The attenuation factor can be derived from equation (F.25)

$$e^{-m_o x} = e^{-\sqrt{z_o y_o}\, x}$$

Also,

$$\sqrt{z_o y_o} = \sqrt{(R_o + sL_o)sC_o}$$

$$= \sqrt{L_o C_o}\, s(1 + R_o/sL_o)^{1/2}$$

$$= \sqrt{L_o C_o}\, s\left[1 + \frac{R_o}{2sL_o}\right]$$

$$= \sqrt{L_o C_o}\, s + \frac{R_o}{2}\sqrt{\frac{C_o}{L_o}}$$

Thus,

$$e^{-\sqrt{z_o y_o}\, x} = e^{-\frac{R_o}{2}\sqrt{\frac{C_o}{L_o}}\, x}\, e^{-\sqrt{L_o C_o}\, sx} \qquad (F.32)$$

The first term which decreases along the line is called the attenuation factor while, the second term which represents the delay is called delay factor.

The particular solution for the transmission line voltage and current is obtained by introducing boundary conditions of the line in equations (F.26) and (F.27). These boundary conditions are, at the sending end i.e. at $x = 0$

$$[E] = [E_o] \quad \text{and} \quad [I] = [I_o]$$

while at the receiving end, i.e. at x = l,

$$[E] = [V] \quad \text{and} \quad [I] = [I_l]$$

Thus, the voltages and currents at the sending and receiving ends are,

$$[E_o] = [T][K_1] + [T][K_2]$$

$$[I_o] = [T][Z]^{-1}[K_1] - [T][Z]^{-1}[K_2] \tag{F.33}$$

$$[V] = [T][K_1 e^{-ml}] + [T][K_2 e^{ml}]$$

$$[I_l] = [T][Z]^{-1}[K_1 e^{-ml}] - [T][Z]^{-1}[K_2 e^{ml}] \tag{F.34}$$

Let,

$$[A] = \begin{bmatrix} A_{1a} \\ A_{1b} \\ A_{1c} \end{bmatrix} = \begin{bmatrix} K_{1a} e^{-m_o l} \\ K_{1b} e^{-m_1 l} \\ K_{1c} e^{-m_1 l} \end{bmatrix} \tag{F.35}$$

and

$$[B] = \begin{bmatrix} B_{2a} \\ B_{2b} \\ B_{2c} \end{bmatrix} = \begin{bmatrix} K_{2a} e^{m_o l} \\ K_{2b} e^{m_1 l} \\ K_{2c} e^{m_1 l} \end{bmatrix} \tag{F.36}$$

from which we can write,

$$[K_2] = \begin{bmatrix} K_{2a} \\ K_{2b} \\ K_{2c} \end{bmatrix} = \begin{bmatrix} B_{2a}e^{-m_o l} \\ B_{2b}e^{-m_1 l} \\ B_{2c}e^{-m_1 l} \end{bmatrix} \qquad (F.37)$$

Finally, the voltage and current at the sending and receiving ends of the line can be written in a simplified form as;

$$\begin{aligned} [E_o] &= [T][K_1] + [T][K_2] \\ [I_o] &= [T][Z]^{-1}[K_1] - [T][Z]^{-1}[K_2] \end{aligned} \qquad (F.38)$$

and

$$\begin{aligned} [V] &= [T][A] + [T][B] \\ [I_1] &= [T][Z]^{-1}[A] - [T][Z]^{-1}[B] \end{aligned} \qquad (F.39)$$

From equations (F.32), (F.35) and (F.37), the following expressions can be written,

$$\begin{aligned} A_{1a}(s) &= K_{1a}(s)\, e^{-\frac{R_o}{2}\sqrt{\frac{C_o}{L_o}}\, l}\, e^{-\sqrt{L_o C_o}\, ls} \\ A_{1b}(s) &= K_{1b}(s)\, e^{-\frac{R_1}{2}\sqrt{\frac{C_1}{L_1}}\, l}\, e^{-\sqrt{L_1 C_1}\, ls} \\ A_{1c}(s) &= K_{1c}(s)\, e^{-\frac{R_1}{2}\sqrt{\frac{C_1}{L_1}}\, l}\, e^{-\sqrt{L_1 C_1}\, ls} \end{aligned} \qquad (F.40)$$

and

$$K_{2a}(s) = B_{2a}(s)\, e^{-\frac{R_o}{2}\sqrt{\frac{C_o}{L_o}}\,l}\, e^{-\sqrt{L_oC_o}\,ls}$$

$$K_{2b}(s) = B_{2b}(s)\, e^{-\frac{R_1}{2}\sqrt{\frac{C_1}{L_1}}\,l}\, e^{-\sqrt{L_1C_1}\,ls} \qquad \text{(F.41)}$$

$$K_{2c}(s) = B_{2c}(s)\, e^{-\frac{R_1}{2}\sqrt{\frac{C_1}{L_1}}\,l}\, e^{-\sqrt{L_1C_1}\,ls}$$

Taking the inverse Laplace transform,

$$a_{1a}(t) = \alpha_o\, k_{1a}(t - T_o)\, U\,(t - T_o)$$

$$a_{1b}(t) = \alpha_1\, k_{1b}(t - T_1)\, U\,(t - T_1) \qquad \text{(F.42)}$$

$$a_{1c}(t) = \alpha_1\, k_{1c}(t - T_1)\, U\,(t - T_1)$$

and,

$$k_{2a}(t) = \alpha_o\, b_{2a}(t - T_o)\, U\,(t - T_o)$$

$$k_{2b}(t) = \alpha_1\, b_{2b}(t - T_c)\, U\,(t - T_1) \qquad \text{(F.43)}$$

$$k_{2c}(t) = \alpha_1\, b_{2c}(t - T_o)\, U\,(t - T_1)$$

where

$$T_o = \sqrt{L_oC_o}\,l\,, \qquad T_1 = \sqrt{L_1C_1}\,l$$

and $\alpha_o = e^{-\frac{R_o}{2}\sqrt{\frac{C_o}{L_o}}\,l}$, $\alpha_1 = e^{-\frac{R_1}{2}\sqrt{\frac{C_1}{L_1}}\,l}$

This presence of delay factor in the above equations (F.42) and (F.43) will be of importance in the solution of transmission line problem.

APPENDIX G

DERIVATION OF MATRICES $k_1(t)$ AND $b_2(t)$ FOR DIFFERENT SYSTEM CONDITIONS

The evaluation of matrix $[k_1(t)]$ depend upon the system condition existing at the sending end and $[b_2(t)]$ depends upon the system conditions existing at the receiving end of the line. The expression for these matrices under different system conditions are derived as outlined.

Case (1) Unloaded Line without Source Impedence taken into Account:

This situation is represented in Figure 3.2. Here, the receiving end line voltages are equal to the source voltages and the receiving end currents are zero, i.e.

$$[E_o(t)] = [E_g(t)]$$

where $[E_g(t)]$ is the source voltage matrix and is given by

$$[E_g(t)] = \begin{bmatrix} E_{ga}(t) \\ E_{gb}(t) \\ E_{gc}(t) \end{bmatrix} = \begin{bmatrix} E_{gm} \sin(wt + \emptyset) \\ E_{gm} \sin(wt - 120° + \emptyset) \\ E_{gm} \sin(wt + 120° + \emptyset) \end{bmatrix} \quad (G.1)$$

where E_{ga}, E_{gb} and E_{gc} are the source voltages of phase a, b and c respectively and $\emptyset$ is the angle of switching of phase 'a' at t = 0.

The expression for the matrices $[k_1(t)]$ and $[b_2(t)]$ get from equations (3.8) and (3.9) will be of the form

$$[k_1(t)] = [T]^{-1} [E_g(t)] - [k_2(t)] \quad (G.2)$$

and $$[b_2(t)] = [a_1(t)] \qquad (G.3)$$

Case (2) Unloaded Line with Source Impedance:

These system conditions are represented in Figure 3.3. At the receiving end, the system boundary conditions are identical as in the case (1). However, at the sending end, the line is connected to the source through a series impedance which consist of inductance L_g and a resistance R_g.

Referring to Figure 3.3 the source voltage matrix can be written as

$$[E_g(t)] = [L_g]\frac{d}{dt}[I_o(t)] + [R_g][I_o(t)] + [E_o(t)] \qquad (G.4)$$

where, source inductance matrix

$$[L_g] = \begin{bmatrix} L_{g1} & 0 & 0 \\ 0 & L_{gb} & 0 \\ 0 & 0 & L_{gc} \end{bmatrix}$$

Here, L_{ga}, L_{gb} and L_{gc} represent source inductances of phase a, b and c respectively.

Source resistance matrix is given by

$$[R_g] = \begin{bmatrix} R_{ga} & 0 & 0 \\ 0 & R_{gb} & 0 \\ 0 & 0 & R_{gc} \end{bmatrix}$$

where R_{ga}, R_{gb} and R_{gc} are source resistances of phases a, b and c respectively.

Substituting equations (3.1) and (3.2) in equation (G.4) we get,

$$[E_g(t)] = [L_g][T][Z]^{-1}\left\{\frac{d}{dt}[k_1(t)] - \frac{d}{dt}[k_2(t)]\right\}$$

$$+ [R_g][T][Z]^{-1}\{[k_1(t)] - [k_2(t)]\}$$

$$+ [T][k_1(t)] + [T][k_2(t)] \qquad (G.5)$$

By suitably manipulating equation (G.5), we get,

$$\frac{d}{dt}[k_1(t)] = \frac{d}{dt}[k_2(t)] + [\gamma][T]^{-1}[E_g(t)]$$

$$+ [\gamma][W][k_1(t)] + [\gamma][X][k_2(t)] \qquad (G.6)$$

where $[\gamma] = [[T]^{-1}[L_g][T][Z]^{-1}]^{-1}$

$$[W] = [[T]^{-1}[R_g][T][Z]^{-1} + [U]] \qquad (G.7)$$

$$[X] = [[T]^{-1}[R_g][T][Z]^{-1} - [U]]$$

and $[U]$ = diagonal unit matrix.

The expression for $[b_2(t)]$ will be of the same form as given in equation (G.2). The differential equations in (G.6) are solved numerically by Euler's predictor-corrector formula [22].

Case (3) Resistive Load with Source Impedance:

The system condition in this case is shown in Figure 3.9. At the sending end, system boundary conditions are identical as in case (2). At the receiving end, the transmission line is terminated with a resistive load. The receiving end voltages and current are related by

$$[V] = [R][I_1] \qquad (G.8)$$

Here load resistance matrix

$$[R] = \begin{bmatrix} R_a & 0 & 0 \\ 0 & R_b & 0 \\ 0 & 0 & R_c \end{bmatrix} \qquad (G.9)$$

where, R_a, R_b and R_c are the resistive load at phase a, b and c respectively.

Now, by substituting the expression for $[V(t)]$ and $[I_1(t)]$ from equations (3.3) and (3.4) in equation (G.8), we get

$$[T][a_1(t)] + [T][b_2(t)] = [R][T][Z]^{-1}\,[a_1(t)] - [R][T][Z]^{-1}\,[b_2(t)]$$

By suitably manipulating the above equation we get,

$$[b_2(t)] = [[T]^{-1}\,[R][T][Z]^{-1} + [U]]^{-1} \times [[T]^{-1}\,[R][T][Z]^{-1} - [U]]\,[a_1(t)] \qquad (G.10)$$

The expression for $[k_1(t)]$ will be of the form as given in equation (G.6).

Case (4) Inductive Load with Source Impedance:

The equivalent circuit of inductive load termination with source impedance taken into consideration is shown in Figure 3.10. The sending end system conditions are same as in case (2). The receiving end voltages and currents are related as follows:

$$[V_o(t)] = [L]\,\frac{d}{dt}\,[I_1(t)] + [R]\,[I_1(t)] \qquad (G.11)$$

Here load inductance matrix is defined as

$$[L] = \begin{bmatrix} L_a & 0 & 0 \\ 0 & L_b & 0 \\ 0 & 0 & L_c \end{bmatrix}$$

where L_a, L_b and L_c are inductance of loads on phases a, b and c respectively. The expression for matrix [R] is same as given in equation (G.9). Substituting the expression of $I_1(t)$ and $V(t)$ from equations (3.3) and (3.4) in equation (3.11), we get,

$$[T][a_1(t)] + [T][b_2(t)] = [L][T][Z]^{-1} \{\frac{d}{dt}[a_1(t)] - \frac{d}{dt}[b_2(t)]\}$$

On rearranging the terms we get,

$$\frac{d}{dt}[b_2(t)] = \frac{d}{dt}[a_1(t)] + [J][M][a_1(t)] - [J][N][b_2(t)] \qquad (G.12)$$

where $[J] = [[T]^{-1}[L][T][Z]^{-1}]^{-1}$

$[M] = [[T]^{-1}[R][T][Z]^{-1} - [U]]$

$[N] = [[T]^{-1}[R][T][Z]^{-1} + [U]]$

The differential equations in (G.12) are then solved by using Euler's predictor-corrector formula [22].